Spring 2018

Characterization of ionic liquid monopropellants for a multi-mode propulsion system

Alex J. Mundahl

Department:

CHARACTERIZATION OF IONIC LIQUID MONOPROPELLANTS FOR A MULTI-MODE PROPULSION SYSTEM

by

ALEX JEFFREY MUNDAHL

A THESIS

Presented to the Faculty of the Graduate School of the

MISSOURI UNIVERSITY OF SCIENCE AND TECHNOLOGY

In Partial Fulfillment of the Requirements for the Degree

MASTER OF SCIENCE IN AEROSPACE ENGINEERING

2018

Approved by

Joshua L. Rovey, Advisor
Henry Pernicka
David Riggins

PUBLICATION THESIS OPTION

This thesis consists of the following two articles, formatted in the style used by the Missouri University of Science and Technology:

Paper I: Pages 6-49 have been presented at a Joint Propulsion Conference

Paper II: Pages 50-73 are intended for submission to the Journal of Propulsion and Power

ABSTRACT

Multi-mode micropropulsion is a potential game-changing technology enabling rapidly composable small satellites with unprecedented mission flexibility. Maximum mission flexibility requires one shared propellant between the chemical and electric systems. A deep eutectic 1:2 molar ratio mixture of choline-nitrate and glycerol ([Cho][NO_3] – glycerol) is investigated as a fuel component in a binary mixture propellant for such a multi-mode micropropulsion. Specifically, binary mixtures of the novel ionic liquid fuel with hydroxyl-ammonium nitrate (HAN) and ammonium nitrate (AN) are considered and compared against the previously investigated propellant [Emim][$EtSO_4$]-HAN. Chemical rocket performance simulations predict this new propellant to have higher performance at lower combustion temperature, relaxing catalyst melting temperature requirements and making it a promising alternative. A qualitative investigation of synthesized propellants on a hot plate in atmosphere indicates the AN mixtures are significantly less reactive, and are therefore not investigated further. Quantitative reactivity studies using a microreactor indicate both 65:35% and 80:20% by mass [Cho][NO_3] – glycerol to HAN propellants have a decomposition temperature 26-88% higher than [Emim][$EtSO_4$]-HAN, depending on the catalyst material. The results indicate [Emim][$EtSO_4$]-HAN with platinum catalyst is still most promising as a multi-mode micropropulsion propellant. Also, the linear burn rate of this monopropellant is determined to aid design of the microtube catalytic chemical thruster. With the design pressure of 1.5 MPa the linear burn rate of this propellant used for designing the multi-mode propulsion system is 26.4 mm/s. Based on this result, the minimum flow rate required is 0.31 mg/s for a 0.1 mm inner diameter feed tube and 3180 mg/s for a 10 mm inner diameter feed tube.

ACKNOWLEDGMENTS

First and foremost, I would like to thank my advisor, Dr. Josh Rovey, for believing in me, and providing me with an immense number of opportunities to learn and grow outside of the classroom. Through these opportunities and other interactions, he has inspired me to push myself to be the best I can become both academically and professionally. I will always appreciate the time I have spent under his supervision, and I look forward to our future collaborations. I would like to thank my committee members Dr. Henry Pernicka and Dr. David Riggins. Their counsel has helped me greatly in determining my path, their instruction through classes helped fuel my passion for Aerospace Engineering, and their advice on this work has been invaluable. I would also like to thank the Office of Graduate Studies for providing me with the Chancellor's Distinguished Fellowship, and an opportunity to pursue my graduate education.

I would also like to thank Durgesh Wagle from the Ionic Liquid Laboratory at the University of Missouri – Columbia for your diligent work and assistance with developing Ionic Liquids for me to test. Huge thanks are due to Dr. Klaus Woelk and Ming Huang in the Chemistry Department of Missouri S&T for testing propellant samples using NMR Spectroscopy, and for assisting us interpret the results. A great many thanks go to the machinists of the MAE department for your assistance and advice. Thank you to my colleagues in the Aerospace Plasma Laboratory for your help and assistance, specifically Mitch, Jakyob, and Paul for your support during our long work sessions and stress relieving conversations. Special thanks to Evan for your continuous reassurance, and I would like to thank my family for all the support they have provided me over the past several years. Without them I would not be where I am today.

TABLE OF CONTENTS

Page

LIST OF ILLUSTRATIONS

Page

PAPER I

PAPER II

LIST OF TABLES

Page

PAPER I

PAPER II

NOMENCLATURE

Symbol	Description
a_x	Thermocouple Voltage to Temperature Coefficient, [$^oC/V^x$]
$C_{p,i}$	Specific heat with respect to constant pressure of species i, [J/kg-K]
$\frac{dT}{dt}$	Total change in temperature with respect to time, [K/s]
D_c	Diameter of propellant container [cm]
I	Current, [A]
I_{sp}	Specific Impulse, [sec]
K	Electrical conductivity, [S/m]
L	Distance between electrical leads connected to the foil, [mm]
m_p	mass of propellant used [g]
MW	Molecular weight, [g/mol]
N_i	Number of moles of species i, [mol]
$\dot{Q}$	rate of heat transferred to the system due to electrical heating and thermal losses, [W]
$\dot{Q}"$	Heat flux per unit area of foil exposed to propellant, [W/mm^2]
r_A	Arrhenius-type reaction rate, [mol/m^3-s]
r_b	linear burn rate [mm/s]
r_{holder}	Propellant Holder internal radius, [mm]
t	time, [sec]
T_c	Combustion Temperature, [K]
T_{decomp}	Onset decomposition temperature, [^oC]
t_f	Foil thickness, [mm]
T_m	Melting Temperature, [K]
$\dot{T}_E$	Electrical heating rate, [K/s]
$\dot{T}_S$	Self-heating rate, [K/s]
V	Volume of reactor, [m^3]

w	Foil Width, [mm]
γ	Surface tension, [dyn/cm]
ΔH_f^o	Enthalpy of Formation, [kJ/mol]
ΔH_{Rx}	Enthalpy of reaction, [J/mol]
Δt	change in time [s]
Δx	change in position [mm]
η	Viscosity, [cP]
κ	Thermal conductivity, [W/m-K]
ρ_d	Density, [g/cm^3]
ρ_e	Electrical resistivity, [Ω-mm]
ρ_p	density of propellant used [g/cm^3]

SECTION

1. INTRODUCTION

This thesis displays work on characterizing ionic liquid monopropellants for a developing multi-mode micropropulsion system. The multi-mode micropropulsion system under development can perform in both a chemical mode and an electric electrospray mode. This system also utilizes catalytic microtubes and a compatible monopropellant to enhance the thruster's performance. The intent of this work is to compare multiple ionic liquids, regardless of the literature data available, to determine an optimal ionic liquid monopropellant for this multi-mode propulsion system. The chosen ionic liquid monopropellant's linear burning rate is also determined to obtain an estimate of the minimum mass flow rate required for this system during the chemical mode operation.

One paper presented at an aerospace conference and another prepared for publication in an aerospace journal are provided to perform this analysis. The first paper specifies each ionic liquid tested, their synthesis processes, and analyzes the decomposition properties of these propellants to determine which propellants require further analysis. The second paper details the linear burn rate results for the chosen ionic liquid monopropellant, and what an estimate for the minimum flow rate required during the chemical mode operations would be. Preceding these papers is an introduction to multi-mode micropropulsion, ionic liquid monopropellants, and the driving motivations for this research.

1.1. MULTI-MODE PROPULSION

Multi-mode propulsion is the use of two or more separate propulsive modes on a single spacecraft. Recently proposed systems make use of a high-specific impulse, usually electric mode, and a high-thrust, usually chemical mode. This can be beneficial in two primary ways: an increase in mission flexibility,[1-6] and the potential to design a more efficient orbit using the two systems compared to a single chemical or electric mode.[7-10] The increase in mission flexibility is achieved due to the availability of the two differing propulsive maneuvers to the mission designer at any point during the mission. This allows for drastic changes to the mission thrust profile at virtually any time before or even after launch without the need to integrate an entirely new propulsion system. Additionally, it has been shown that, under certain mission scenarios, it is beneficial in terms of spacecraft mass savings, or deliverable payload, to utilize separate high-specific impulse and high-thrust propulsion systems even if there is no shared hardware or propellant.[7, 8] However, even greater mass savings can be realized by using a shared propellant and/or hardware even if the thrusters perform lower than state-of-the-art in either mode.[3, 11] In order to realize the complete potential of a multi-mode propulsion system, it is necessary to utilize one shared propellant for both modes; this allows for a large range of possible maneuvers while still allowing for all propellant to be consumed regardless of the specific choice or order of maneuvers.[5, 6]

Small spacecraft have seen a growth in popularity, specifically microsatellites (10-100 kg) and nanosatellites (1-10 kg), including the subset of CubeSats. Many different types of thrusters have been proposed to meet the stringent mass and volume requirements placed on spacecraft of this type. Electrospray propulsion systems are good options for

micropropulsion, and have been selected for such applications.[12, 13] Many different chemical propulsion systems have also been proposed, including a chemical microtube.[14-16] This propulsion system utilizes a heated tube with a typical diameter of 1 mm or less that could consist of a catalytic surface material. Additionally, capillary type emitters used for an electrospray propulsion system can be roughly the same diameter tube, and there is therefore no fundamental reason why this geometry could not be shared within a multi-mode propulsive system.[17, 18]

1.2. IONIC LIQUID MONOPROPELLANTS

Recent efforts in developing propellants for space vehicles have focused on finding a high-performance, low-toxicity propellant replacement for traditional, but highly toxic options. Hydrazine has been chosen for use in gas generators and spacecraft monopropellant thrusters due to its storability and favorable decomposition characteristics in providing relatively high performance.[19] However, hydrazine is difficult from a handling perspective because it is highly toxic. A large amount of the research toward a hydrazine replacement is focused on energetic ionic liquids. An energetic ionic liquid is a molten salt with an energetic functional group capable of rapid exothermic decomposition. Energetic salts that have been studied for such purposes include ammonium dinitramide (ADN), hydrazinium nitroformate (HNF), and hydroxylammonium nitrate (HAN).[19-23] Typically, these salts are mixed with compatible fuels to improve the performance characteristics of the produced propellant. However, the high combustion temperatures for these energetic monopropellants have been the main limitation in their practical use in spacecraft thrusters, but recent research in thermal management and materials have

mitigated some issues, and multiple flight tests are scheduled, or have already been conducted.[12, 24, 25] These propellants perform well in chemical thrusters, but they are fundamentally unable to perform as an electrospray propellant due to their water content or other volatile component. To overcome this, monopropellants were developed, synthesized, and shown to be capable of high performance in an electrospray thruster.[11, 26]

Previous work has developed two propellants that can function as both a chemical monopropellant and an electric electrospray propellant.[11] These monopropellants have been previously synthesized and assessed for thermal and catalytic decomposition within a microreactor[26] and for performance in an electrospray emitter.[27] One of the monopropellant combinations, a mixture of 1-ethyl-3-methylimidazolium ethyl sulfate ([Emim][EtSO4]) and hydroxylammonium nitrate (HAN), has also been further analyzed to determine its decomposition characteristics on relevant catalytic surfaces,[26, 28] and its linear burn rate has been measured at pressures relevant to typical monopropellant thruster operation.[29] Challenges with this propellant include high combustion temperature required for high performance (2700 K for 300 sec Isp, 1800 K for 250 sec Isp with a nozzle) and drying HAN to reduce the water (volatile) content of the propellant.

1.3. PURPOSE

New and improved multi-mode propellants that overcome these challenges may be possible by designing ionic liquids based on knowledge gained from the previous propellants tested. This is one of the objectives of the present work. Specifically, a novel ionic liquid fuel, choline nitrate – glycerol ([Cho][NO3] – glycerol), and created mixtures

of it with oxidizers ammonium nitrate (AN) and HAN. In the following analysis, the synthesis process for these new propellants is described. Additionally, the predicted chemical propulsion performance of these new propellants is compared to our existing multi-mode propellant. Then, the new propellants are tested on a spot-plate and within a microreactor to assess their decomposition on common catalyst materials. These results are also compared with previous multi-mode propellants. From these results, a propellant is chosen for further analysis.

The linear burn rate of the propellant, used at the thruster's anticipated operating pressures, is a useful parameter in the design of the system, both for thruster operation and flashback prevention. The linear burn rate has been studied previously for monopropellants, including HAN-based monopropellants.[30-32] This thesis presents results on the experimental determination and assessment of the linear burn rate characteristics of the [Emim][EtSO4]-HAN propellant at various pressures using a pressurized strand burner setup. These measurements, taken together, can be used to aid in the design and optimization of a catalytic microtube thruster. Finally, these results are discussed with respect to microtube thruster parameters.

PAPER

I. CHARACTERIZATION OF A NOVEL IONIC LIQUID MONOPROPELLANT FOR MULTI-MODE PROPULSION

Alex J. Mundahl[1], Steven P. Berg[2], Joshua L. Rovey[3], Ming Huang[4], and Klaus Woelk[5]
Missouri University of Science and Technology, Rolla, Missouri 65409

and

Durgesh V. Wagle[6] and Gary Baker[7]
University of Missouri-Columbia, Columbia, Missouri 65211

ABSTRACT

A deep eutectic 1:2 molar ratio mixture of choline-nitrate and glycerol [Cho][NO_3] – glycerol is investigated as a fuel component in a binary mixture propellant for multi-mode micropropulsion. Specifically, binary mixtures of the novel ionic liquid fuel with hydroxyl-ammonium nitrate (HAN) and ammonium nitrate (AN) are considered and compared against our previously investigated propellant [Emim][$EtSO_4$]-HAN. Chemical

---

[1] Graduate Research Assistant, Aerospace Plasma Laboratory, Mechanical and Aerospace Engineering, 160 Toomey Hall, 400 W. 13th Street, Student Member AIAA.
[2] Post Doctoral Fellow, Aerospace Plasma Laboratory, Mechanical and Aerospace Engineering, 160 Toomey Hall, 400 W. 13th Street, Student Member AIAA.
[3] Associate Professor/Associate Chair for Graduate Affairs, Mechanical and Aerospace Engineering, 194C Toomey Hall, 400 W. 13th Street, Associate Fellow AIAA.
[4] Graduate Research Assistant, Chemistry Department, 342 Schrenk Hall, 400 W 11th Street, and AIAA Member Grade.
[5] Associate Chair, Associate Professor, Chemistry Department, 321A Schrenk Hall, 400 W 11th Street , and AIAA Member Grade.
[6] Graduate Research Assistant, Department of Chemistry, 125 Chemistry Building, 601 S College Avenue, and AIAA Member Grade for third author.
[7] Associate Professor, Department of Chemistry, 125 Chemistry Building, 601 S College Avenue, and AIAA Member Grade for third author.

rocket performance simulations predict this new propellant to have higher performance (280 vs. 250 sec specific impulse) at lower combustion temperature (1300 vs. 1900K), relaxing catalyst melting temperature requirements and making it a promising alternative. Qualitative experimental investigation of synthesized propellants on a hot plate in atmosphere indicate the AN mixtures are significantly less reactive, and are therefore not investigated further. Quantitative reactivity studies using a microreactor indicate that both 65:35% and 80:20% by mass [Cho][NO_3] – glycerol to HAN propellants have a decomposition temperature 26-88% higher than [Emim][$EtSO_4$]-HAN, depending on the catalyst material. Additionally, the decomposition rate (or self-heating rate) was 2 to 17 times slower for [Cho][NO_3] – glycerol – HAN on titanium and platinum catalysts, but the 65:35% propellant decomposition rate was approximately 10 $^oC/s$ (37%) faster on rhenium. It was also observed that propellants with the novel ionic liquid fuel contain endothermic reaction steps, and therefore higher input heat flux was required to maintain a temperature rise. Overall the results indicate [Emim][$EtSO_4$]-HAN with platinum catalyst is still most promising as a multi-mode micropropulsion propellant.

NOMENCLATURE

a_x = Thermocouple Voltage to Temperature Coefficient, [$^oC/V^x$]

$\frac{dT}{dt}$ = Total change in temperature with respect to time, [K/s]

T_c = Combustion Temperature, [K]

T_{decomp} = Onset decomposition temperature, [^oC]

T_m = Melting Temperature, [K]

ρ_d = Density, [g/cm^3]

ρ_e = Electrical resistivity, [Ω-mm]

ΔH_f^o = Enthalpy of Formation, [kJ/mol]

η = Viscosity, [cP]

K = Electrical conductivity, [S/m]

γ = Surface tension, [dyn/cm]

I_{sp} = Specific Impulse, [sec]

κ = Thermal conductivity, [W/m-K]

T_m = Melting Temperature, [K]

MW = Molecular weight, [g/mol]

$\dot{Q}$ = rate of heat transferred to the system due to electrical heating and thermal losses, [W]

ΔH_{Rx} = Enthalpy of reaction, [J/mol]

r_A = Arrhenius-type reaction rate, [mol/m^3-s]

V = Volume of reactor, [m^3]

N_i = Number of moles of species i, [mol]

$C_{p,i}$ = Specific heat with respect to constant pressure of species i, [J/kg-K]

$\dot{T}_E$ = Electrical heating rate, [K/s]

$\dot{T}_S$ = Self-heating rate, [K/s]

$\dot{Q}$" = Heat flux per unit area of foil exposed to propellant, [W/mm^2]

I = Current, [A]

L = Distance between electrical leads connected to the foil, [mm]

w = Foil Width, [mm]

t = time, [sec]

t_f = Foil thickness, [mm]

r_{holder} = Propellant Holder internal radius, [mm]

1. INTRODUCTION

Multi-Mode propulsion is the use of two or more separate propulsive modes on a single spacecraft. Recently proposed systems make use of a high-specific impulse, usually electric mode, and a high-thrust, usually chemical mode. This can be beneficial in two primary ways: an increase in mission flexibility,[1, 3-6, 33] and the potential to design a more efficient orbit using the two systems compared to a single chemical or electric mode.[7-10] The increase in mission flexibility is achieved due to the availability of the two differing propulsive maneuvers to the mission designer at any point during the mission. This allows for drastic changes to the mission thrust profile at virtually any time before or even after launch without the need to integrate an entirely new propulsion system. Additionally, it has been shown that, under certain mission scenarios, it is beneficial in terms of spacecraft mass savings, or deliverable payload, to utilize separate high-specific impulse and high-thrust propulsion systems even if there is no shared hardware or propellant.[7, 8] However, even greater mass savings can be realized by using a shared propellant and/or hardware even if the thrusters perform lower than state-of-the-art in either mode.[3, 11] In order to realize the complete potential of a multi-mode propulsion system, it is necessary to utilize one shared propellant for both modes; this allows for a large range of possible maneuvers while still allowing for all propellant to be consumed regardless of the specific choice or order of maneuvers.[5, 6]

One promising approach to multi-mode propulsion is the combination of a chemical monopropellant microtube thruster with an electric electrospray thruster.[26, 27] This type of system would have shared propellant and shared hardware, and would be ideally suited for micropropulsion applications.[5] The system is a single propulsion system (one

propellant tank, one set of feed lines/valves, one thruster) that can be operated in either high-thrust low-specific impulse chemical mode or low-thrust high-specific impulse electric mode. A microtube/emitter (~0.1-mm-diam.) is fed with a novel multi-mode propellant blend. If the tube is heated (160ºC) the propellant catalytically and exothermically decomposes to produce high-temperature gaseous exhaust species with a specific impulse of 180 sec (theoretically 250 sec if a nozzle is used). If instead a potential difference (~3000 V) is applied between the tube and an extraction electrode, ions and charged droplets are extracted from the propellant with a specific impulse of >780 sec, this is the optimum electric specific impulse for the given chemical specific impulse. A collection or array of microtubes/emitters is a thruster.

Our previous work has developed two propellants that can function as both a chemical monopropellant and an electric electrospray propellant.[11] These monopropellants have been previously synthesized and assessed for thermal and catalytic decomposition within a microreactor,[26] and for performance in an electrospray emitter.[27] One of the monopropellant combinations, a mixture of 1-ethyl-3-methylimidazolium ethyl sulfate ([Emim][$EtSO_4$]) and hydroxylammonium nitrate (HAN), has also been further analyzed to determine its decomposition characteristics on relevant catalytic surfaces,[26, 34] and its linear burn rate has been measured at pressures relevant to typical monopropellant thruster operation.[29] Challenges with this propellant include high combustion temperature required for high performance (2700 K for 300 sec I_{sp}, 1800 K for 250 sec I_{sp} with a nozzle) and drying HAN to reduce the water (volatile) content of the propellant.

New and improved multi-mode propellants that overcome these challenges may be possible by designing ionic liquids based on knowledge gained from the previous propellants tested. This is the focus of the present work. Specifically, we have designed and synthesized a new ionic liquid fuel, choline nitrate – glycerol ([Cho][NO_3] – glycerol), and created mixtures of it with oxidizers ammonium nitrate (AN) and HAN. The following sections describe the predicted chemical propulsion performance of these new propellants with comparison to our existing multi-mode propellant. Then the synthesis process for these new propellants is described. Additionally, the new propellants are tested on a spot-plate and within a microreactor to assess their decomposition on common catalyst materials. These results are also compared with previous multi-mode propellants.

2. PROPELLANTS DESCRIPTION

Four different ionic liquids are used in this work, two fuels and two oxidizers: [Emim][$EtSO_4$] and [Cho][NO_3] – glycerol, and hydroxylammonium nitrate (HAN) and ammonium nitrate (AN), respectively. The chemical structure of each of these ionic liquids is provided in Figure 1. The available properties for these ionic liquids are given in Table 1. A propellant is the combination of one fuel with one oxidizer (creating a pre-mixed bipropellant), and propellants with different fuel-oxidizer ratio are synthesized and tested. Our previous work has studied mixtures of [Emim][$EtSO_4$] with HAN. The main focus of this work is comparison of those results with mixtures of [Cho][NO_3] – glycerol with HAN and [Cho][NO_3] – glycerol with AN.

The new ionic liquid [Cho][NO_3] – glycerol has been designed based on known desirable properties for a multi-mode propellant. Specific desirable properties for a monopropellant-electrospray multi-mode propulsion system include a high density (> 1 g/cm^3), low melting temperature (T_m < 2^oC), high heat of formation (> 100 kJ/mol), low viscosity (< 100 cP), high electrical conductivity (> 0.9 S/m), and high surface tension (> 37 dyn/cm). Additionally, for monopropellant operation it is desirable to have sufficient oxygen to combust to gaseous products CO, N_2, and H_2. An increase in the amount of hydrogen and oxygen within the ionic liquid can lead to increased chemical performance. Based on these requirements, and using their years of experience studying and designing ionic liquids, the researchers of the University of Missouri-Columbia Ionic Liquid Research Laboratory created the deep-eutectic mixture [Cho][NO_3] – glycerol, which is a 1:2 mole ratio of choline nitrate and glycerol. This particular mixture includes an ammonium cation, a nitrate anion, and seven times the number of hydroxyl groups when compared with the previously tested [Emim][$EtSO_4$] – HAN mixture. The extra hydroxyl groups are a source of oxygen, which could enhance the combustion properties of this fuel during chemical mode operation.

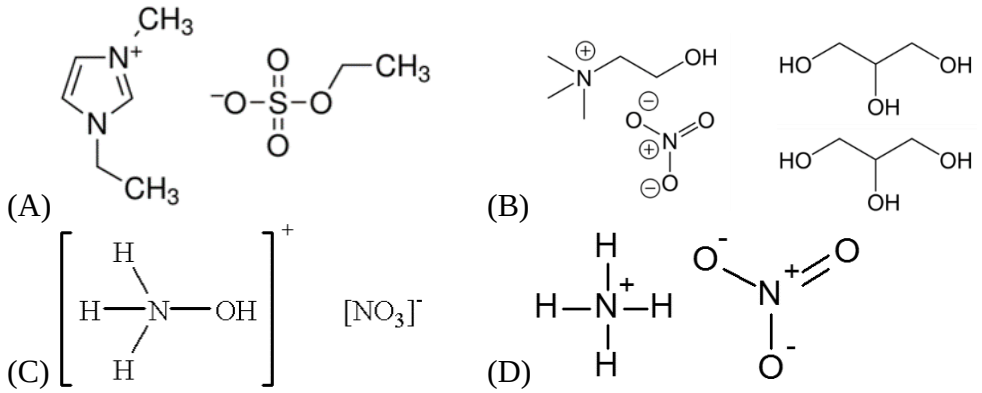

Figure 1 Chemical Structure of ionic liquid compounds used in this study. (A) [Emim][$EtSO_4$], (B) [Cho][NO_3]-glycerol, (C) hydroxylammonium nitrate (HAN), and (D) ammonium nitrate (AN)

Table 1. Physical properties of ionic liquids used in this study

Propellant	**Chemical Formula**	**MW**	**ρ, g/cm^3**	**T_m, ^{o}C**	**ΔH^o_f, kJ/mol**
[Emim][$EtSO_4$]	$C_8H_{16}N_2O_4S_1$	236	1.236	-37	-579.1[35]
[Cho][NO_3]-glyc	$C_{11}H_{30}O_{10}N_2$	350	1.14	-	-
HAN	$N_2H_4O_4$	96	1.84	-	-338.7[36]
AN	$N_2H_4O_3$	80	1.725	169.6	-364.8[36]

As shown in Figure 1, [Cho][NO_3]-glyc has a ratio of hydrogen and oxygen atoms to carbon atoms of 40:11, or 3.6:1. Whereas [Emim][$EtSO_4$] has a ratio of only 20:8, or 2.5:1. These ratios suggest [Cho][NO_3]-glyc will require less oxygen, and therefore less oxidizer to have a balanced chemical reaction. Table 1 also shows the lack of information available for the novel ionic liquid [Cho][NO_3]-glyc as it is a new ionic liquid that has never been investigated.

3. CHEMICAL EQUILIBRIUM ANALYSIS

Chemical equilibrium analysis was used to predict chemical propulsion performance of propellants. The NASA Chemical Equilibrium with Applications (CEA) computer code was used to perform equilibrium combustion analysis, and predict performance (specific impulse). Binary mixtures of [Emim][$EtSO_4$] with HAN have been previously investigated with results predicting good performance (~250 sec Isp at 41:59% by mass fuel-oxidizer mixture ratio).[11, 37] The focus here is on comparing those previous results with predicted performance of the new [Cho][NO_3] – glycerol fuel when it is mixed with HAN or AN. Hydroxylammonium nitrate has been noted for its solubility in fuels[38] and is the chosen oxidizer from previous studies with [Emim][$EtSO_4$]. Ammonium nitrate, however, is not noted for its solubility, but it was chosen to study its feasibility in replacing HAN as an oxidizer with [Cho][NO_3] – glycerol.

An important input to chemical equilibrium calculations is the heat of formation of the compound. The heat of formation of [Cho][NO_3] – glycerol is unknown. So, the enthalpy of formation for [Emim][$EtSO_4$] and HAN were used as a lower and upper bound, respectively, for the enthalpy of formation of [Cho][NO_3] – glycerol. These values are expected to provide a conservative estimate for two reasons: a lower enthalpy of formation value provides less performance with respect to I_{sp} when compared to larger enthalpy of formation values for propellants of similar empirical structure and formula, and [Emim][$EtSO_4$] has the lowest enthalpy of formation of the ionic liquids considered in previous assessments of ionic liquids for chemical microtube propulsion applications.[11, 37] Therefore, in the following results the *min* results used [Emim][$EtSO_4$] heat of formation for [Cho][NO_3] – glycerol, and the *max* results used HAN heat of formation for

[Cho][NO_3] – glycerol (as shown in Figure 2 and Table 2). Additional inputs to the model were temperature of reactants of 298K, chamber pressure of 300 psi, ambient pressure set to vacuum conditions, nozzle expansion ratio of 50, and the flow was assumed to be frozen after the throat if condensed products were not present. If condensed species were present, a shifting equilibrium assumption through the nozzle must be applied to account for the multi-phase flow. These values are typical values for on-orbit engines.[39]

The specific impulse (I_{sp}), combustion temperature (T_c), and mole fractions of the exhaust species were calculated as a function of percent oxidizer by weight in the binary mixture. These results are shown for each propellant mixture in Figure 2. In Figure 2A the highest I_{sp} performance is obtained at the stoichiometric mixture ratio, which is around 75-80%. However, as seen in Figure 2B, the combustion temperature at these conditions (2500-2900 K) is not feasible with materials, catalysts, and technology currently available. We assume the current catalyst technology limit is 1900 K based on the Swedish green monopropellant thruster.[40] Hence our previous work has focused on a 59% HAN oxidizer – 41% [Emim][$EtSO_4$] fuel mixture since the predicted combustion temperature is 1900 K resulting in 254 sec I_{sp}.

Perhaps the most interesting CEA result is the substantially higher performance predicted for [Cho][NO_3] – glycerol mixtures, with significantly less oxidizer. As Figure **2**A shows, [Cho][NO_3] – glycerol –HAN mixtures have higher specific impulse than [Emim][$EtSO_4$]-HAN for all oxidizer fractions, and [Cho][NO_3] – glycerol–AN mixtures have higher specific impulse for all oxidizer fractions below 67%. These results can be explained by the combustion products in the exhaust plume for [Emim][$EtSO_4$] – HAN and [Cho][NO_3] – Glycerol – HAN shown in Figure 2C and Figure 2D respectively. These

figures show that the exhaust plume of the novel ionic liquid has greater fractions of lower molecular weight products, especially H_2 and CO, while producing up to 30% less excess carbon than the exhaust plume of [Emim][$EtSO_4$] – HAN combustion. These differences in the mole fractions also explain why these mixtures have lower combustion temperatures. Theoretically [Cho][NO_3] – glycerol by itself (0% oxidizer) has an over 10 second higher I_{sp} than the 59% oxidizer [Emim][$EtSO_4$] – HAN mixture used in previous studies. However, as shown in Figure 2D there is excess carbon in the exhaust plume for pure [Cho][NO_3] – glycerol. Excess carbon in the exhaust plume of a multi-mode propulsion system utilizing a chemical microtube mode could cause a blockage within the microtube and should be avoided. Therefore, a non-zero amount of oxidizer (>15%) should be added to reduce excess carbon formation.

Based on the CEA predictions, multiple propellants are selected for further investigation. Specifically, propellants that are mixtures of [Cho][NO_3] – glycerol with HAN and [Cho][NO_3] – glycerol with AN are selected, and these are given in Table 2 (propellants B to E). Table 2 provides the I_{sp}, combustion temperature, and the percent of fuel and oxidizer for each propellant. These new propellants are interesting and desirable because of their high predicted performance (I_{sp} >250 sec, and relatively low combustion temperature T_c <1900 K). These new propellants will be compared against the propellant of our previous work [Emim][$EtSO_4$] – HAN (propellant A). We select propellant B ([Cho][NO_3] – glycerol – HAN at 65:35% by mass, respectively) because the predicted combustion temperature is at the maximum possible catalyst material limit (~1900 K), resulting in a specific impulse of ~280 sec. We select propellants C, D, and E ([Cho][NO_3] – glycerol with 20% HAN, 20% AN, and 10% AN, respectively) because they have no

condensed carbon in the combustion products, equivalent or greater I_{sp} than propellant A, significantly lower combustion temperature (1300 vs 1900 K), and demonstrated dissolution of oxidizer into the fuel. We attempted to synthesize other propellants that were mixtures of [Cho][NO_3] – glycerol with AN at an AN concentration greater than 20% by mass. However, these mixtures did not completely dissolve into a uniform solution, and so were not included for further study. Synthesis of the propellants in Table 2 is described next, followed by qualitative reactivity testing using a spot-plate, and then more detailed and quantitative microreactor testing.

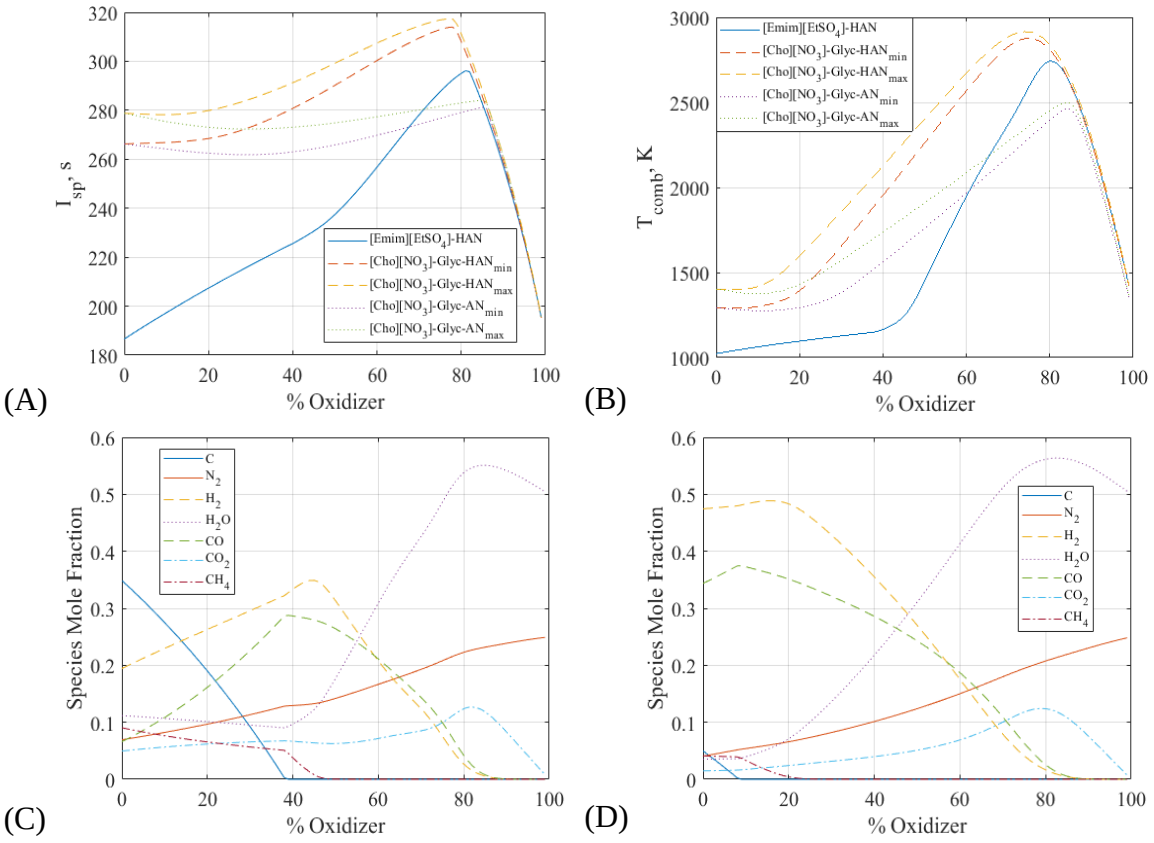

Figure 2. Simulation results for binary mixtures of ionic liquid fuels with HAN or AN oxidizers. (A) specific impulse, (B) combustion temperature, and (C) combustion products for [Emim][$EtSO_4$] – HAN, and (D) combustion products for [Cho][NO_3] – Glycerol – HAN_{max}

Table 2. Summary of binary monopropellant mixtures selected for further experimental analysis with predicted chemical propulsion performance.

Propellant Name	[Cho][NO_3]-glyc ΔH^o_f bound	Fuel	Oxidizer	Fuel %	Oxidizer %	I_{sp}, s	T_c, K
A	N/A	[Emim][$EtSO_4$]	HAN	41	59	254	1900
B	Max	[Cho][NO_3]-glyc	HAN	65	35	287	1991
	Min	[Cho][NO_3]-glyc	HAN	65	35	276	1803
C	Max	[Cho][NO_3]-glyc	HAN	80	20	280	1598
	Min	[Cho][NO_3]-glyc	HAN	80	20	268	1394
D	Max	[Cho][NO_3]-glyc	AN	80	20	273	1429
	Min	[Cho][NO_3]-glyc	AN	80	20	262	1294
E	Max	[Cho][NO_3]-glyc	AN	90	10	275	1375
	Min	[Cho][NO_3]-glyc	AN	90	10	264	1274

4. PROPELLANT SYNTHESIS AND SPECTROSCOPY

The synthesis process for each of the ionic liquids and the resulting propellant mixtures is described. Nuclear magnetic resonance (NMR) spectroscopy measurements are presented showing the propellant composition. Specifically, the water content of HAN-based propellant is a major focus.

4.1. PROPELLANT SYNTHESIS

This section describes the synthesis and preparation of the ionic liquids and propellants used in this study. The synthesis and preparation of the fuel ionic liquids will be described first, then the oxidizers. The prepared fuel and oxidizer ionic liquids are mixed (with a desired mass ratio) to create a propellant (as shown in Table 2). The [Emim][$EtSO_4$] is prepared by drying in vacuum. Specifically, the dilute >99.5% by mass [Emim][$EtSO_4$] (from Sigma Aldrich) is dried under high vacuum (~15μTorr) in a bell-jar chamber with a

cryogenic pump for a minimum of 8 hrs to remove water and volatile impurities. This drying process occurs simultaneously with the drying process of the oxidizer, HAN, and is not completed until the HAN is prepared.

[Cho][NO_3] – glycerol was prepared using a solution of deionized water, choline chloride, and silver nitrate mixed in a round bottom flask with a magnetic stirring bar. This mixture produces the white precipitate silver chloride, and once the precipitate was finished forming, it was filtered out of the solution. The resultant solution was placed under rotary evaporation at 1 mbar at 60 ^{o}C to remove the water from the solution. The resulting precipitate is choline nitrate. Glycerol was then inserted into the round flask with the choline nitrate in a 1:2 mole ratio of choline nitrate to glycerol. Once this new mixture was formed, it was placed under rotary evaporation again for 2 hours. NMR spectroscopy was performed on the initial formulations of this ionic liquid, and will be described in detail below.

Ammonium Nitrate (AN) is stable in its solid form, and is procured from Sigma Aldrich in its solid state. Therefore, the mixtures of AN in [Cho][NO_3] – glycerol were prepared by measuring the mass of solid oxidizer, as indicated in Table 2, and inserting this mass into the [Cho][NO_3] – glycerol liquid.

Hydroxylammonium nitrate (HAN) was prepared three different ways, and we use NMR spectroscopy to qualitatively investigate the resulting water content. The preparation of the three samples is summarized in Table 3. In all cases, dilute (24% by mass) HAN from Sigma Aldrich is used as the starting point. For the first case (HAN-A), a 9.1g sample of dilute HAN-water solution is placed in a vacuum desiccant chamber under rough vacuum (~100mTorr) for approximately two hours. The desiccant was phosphorous

pentoxide. We estimate the sample still had 4.6% by mass water remaining based on the measured mass before and after drying, and assuming no HAN loss during the drying process. For the second case (HAN-B), a similar sample of dilute HAN-water solution was placed in the vacuum desiccant chamber for approximately two hours, but it was then transferred to a high-vacuum (~15 μTorr) bell-jar where it was dried for a further 24 hrs. Additionally, during the high-vacuum drying the sample was stirred occasionally in-situ with a rotation stage. The remaining water content of this sample is unknown, but expected to be non-zero since solid HAN was not obtained. The HAN-B remaining water content is also expected to be less than sample HAN-A due to the longer time in vacuum. For the third case (HAN-C), a similar sample of dilute HAN-water solution was placed in the vacuum desiccant chamber for approximately four hours. It was then transferred to the high-vacuum bell-jar where it was maintained under rough vacuum conditions for 12 hours. It was then subjected to high-vacuum conditions (~15 μTorr) using a cryogenic pump for approximately 16 hours, and then brought back to atmospheric pressure. Isopropyl-alcohol (IPA) was injected into the solution, and it was then placed under high vacuum conditions for another 24 hours. No mechanical agitation/stirring occurred during this synthesis process. This procedure produced solid crystallized HAN. The remaining water content of this sample is unknown, but expected to be very small since solid HAN was formed, and this sample is expected to have the lowest water content, a result qualitatively verified from NMR measurements described below. Table 3 provides a summary of how each of these HAN samples was prepared. Each of these HAN samples was then mixed with [Emim][$EtSO_4$] to create a version of propellant A (Table 2).

Table 3. Preparation of HAN samples.

Sample	[Emim][$EtSO_4$] [%]	HAN [%]	Water [%]	Desiccant Chamber time, hr	Bell-Jar System Time, hr	Rotation Stage?	IPA?
HAN-A	38.9	56.5	4.6	~2	-	No	No
HAN-B	41.3	58.7	unknown	~2	~24	Yes	No
HAN-C	41.4	58.6	unknown	~4	~40	No	Yes

Fuel and oxidizer ionic liquids, prepared as described above, are mixed to form propellants. Each of the HAN samples (HAN-A, B, C) are mixed with [Emim][$EtSO_4$] to create versions of propellant A. [Cho][NO_3] – glycerol is mixed with AN and HAN to create propellants B, C, D, and E (Table 2). The HAN-C preparation method is used for propellants B and C.

4.2. NMR SPECTROSCOPY

Nuclear magnetic resonance (NMR) spectroscopy was performed on the neat ionic liquid [Emim][$EtSO_4$] in aqueous solution, the three [Emim][$EtSO_4$] – HAN propellant samples described in the previous section (Table 3), and [Cho][NO_3] – glycerol. [Emim][$EtSO_4$] in aqueous solution was tested to verify the NMR results agreed with the manufacturer's claim. The three samples of [Emim][$EtSO_4$] – HAN propellant was tested to study the water content of propellant mixtures using HAN prepared according to the three different techniques outlined in Table 3. Water content in multi-mode microtube-electrospray propellant is a concern because water is a volatile impurity. Its presence will not only decrease performance in both chemical microtube (because it reduces combustion temperature) and electric electrospray mode (because it boils off), but can also be

detrimental to achieving stable electric electrospray operation. Therefore, a propellant with no or as little as possible water content is desirable. [Cho][NO_3] – glycerol was tested to verify the synthesis procedure of this novel ionic liquid, and ensure there are no significant impurities.

NMR measurements in aqueous solutions are a standard and information-rich analysis technique in chemistry and related disciplines. ^{1}H NMR chemical shifts reflect the electronic environment of hydrogen nuclei in chemical compounds and thus can be associated with chemical functional groups. The exact chemical-shift position of hydrogen atoms, however, depends not only on the intramolecular electronic environment, but may also be affected by the surrounding solvent and, in case of water as the solvent, by the pH of the solution. It is well known that hydration and hydrogen bonding plays a significant role in the condensed phases of water,[41] and that the chemical shift of a solute will be influenced by these two effects. Furthermore, rapid exchange of hydrogen ions (H^+ ions, i.e., protons) or hydroxide ions (OH^- ions) from the solvent with those at dissolved substrate molecules can lead to a collapse of solvent and solute NMR signals into a single, often broadened, NMR signal at a weighted-average chemical-shift position. Hence, the amount of water and the intensity of hydrogen bonding will influence chemical shift and lineshape of solvent and solute NMR signals in a particular sample. While this is typically seen as a disadvantage in NMR spectroscopy because of the loss of specificity and the loss of the ability to quantify substrates, the relative position and lineshape of averaged, exchangeable hydrogen atoms can still provide useful information when comparing samples with different amounts of residual water.

Samples of neat [Emim][$EtSO_4$] and [Emim][$EtSO_4$]-HAN mixtures were placed into standard 5-mm NMR tubes and investigated with a Bruker AVANCE DRX 200 MHz liquid-state NMR spectrometer. No deuterated solvents (such as D_2O) were added, and the samples investigated without the deuterium field-frequency lock that is typically used to stabilize the magnetic field of NMR spectrometers. ^1H NMR spectra were recorded at room temperature using a 16-scan single-pulse excitation. The pulse angle was set to about p1 = 85° with a relaxation delay of d1 = 5 s between consecutive scans. Standard sample spinning was employed to enhance spectral resolution. Because no field-frequency lock could be used to homogenize the magnetic field, a specially developed magnetic-field shimming procedure was applied to each sample optimizing the free induction decay (FID) performance before conducting NMR experiments. A conventional Fast Fourier Transform (FFT) routine was used to convert FID data to NMR spectra.

Figure 3 shows the 200 MHz ^1H NMR spectrum of a neat [Emim][$EtSO_4$] sample (Sigma Aldrich Co. LLC.) and the assignment of resonance frequencies (NMR signals) to the chemical structure. Six signals are observed for the [Emim] cation (a to f in Figure 3) and two for the [$EtSO_4$] anion (A and B in Figure 3). Small amounts of residual water are identified by a signal at 4.0 ppm in the shoulder of the [Emim] ethyl CH_2-group signal (4.1 ppm). A quantitative signal analysis after deconvolution of the two overlapping signals confirms the manufacturer's claim of about 0.1% by mol residual water in the commercially available product. There are also some unidentified minor impurities (< 0.3% ^1H by mol) observed in the sample (NMR signals at 1.0, 2.0, 2.7, 3.7-3.9, 6.9-7.8, and 8.8 ppm).

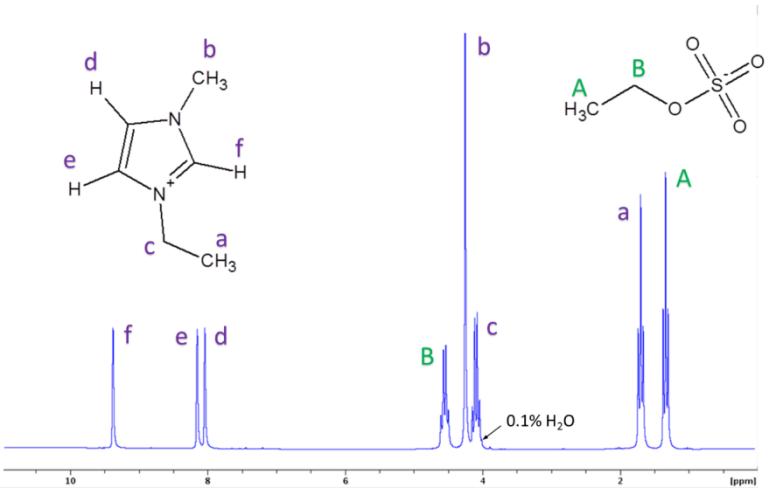

Figure 3. ^{1}H NMR spectrum of neat [Emim][$EtSO_4$] (Sigma Aldrich Co. LLC.)

Figure 4 shows a stacked plot of NMR spectra of the different mixtures of [Emim][$EtSO_4$]-HAN (propellant A) using HAN prepared by different techniques, as described in Table 3. Each of these samples (HAN-A, HAN-B, HAN-C) contain different amounts of residual water due to the HAN preparation process. We expect the water content to decrease from HAN-A to HAN-B to HAN-C, and indeed this is what the NMR spectra confirm. Because no deuterated solvent, and thus no field-frequency lock, was used in this series of experiments, the triplet NMR signal of the [$EtSO_4$] CH_3-group was used as chemical-shift reference (dashed vertical line in Figure 4). While the chemical shifts of the eight [Emim][$EtSO_4$] signals are fairly constant, the HAN and water NMR signals have collapsed into one that moves significantly toward higher ppm values (5.56 ppm, 9.98 ppm and 10.01 ppm in Figure 4a, Figure 4b, and Figure 4c, respectively) with decreasing amounts of residual water. In addition, the linewidth of the collapsed HAN/H_2O signal also depends on the water content; the signal becomes significantly sharper (more narrow) as the water content decreases (57.6 Hz, 11.5 Hz, and 5.7 Hz in Figure 4a, Figure 4b, and Figure 4c, respectively). From this analysis, it follows with great certainty that the amount

of residual water in the sample prepared according to HAN-C (Figure 4c) contains less water than the sample prepared according to HAN-B (Figure 4b).

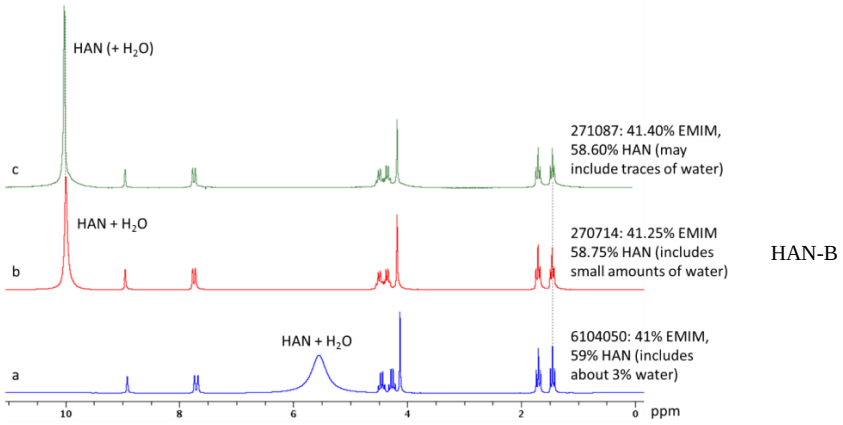

Figure 4. Stacked Plot of NMR Spectra of HAN-[Emim][EtSO4] prepared with the samples of Table 3

NMR analysis was performed on samples of the novel ionic liquid, [Cho][NO_3] – glycerol using the same procedure but a different machine. A Bruker AVANCE III 500 MHz instrument with D_2O was used. The results from this analysis are shown in Figure 5. The peaks in the NMR spectra correspond with the expected chemical structure of [Cho][NO_3] – glycerol, and the peaks are labeled with the corresponding chemical structure. Therefore, the NMR spectra verify that the solution tested is indeed chemically accurate [Cho][NO_3] – glycerol.

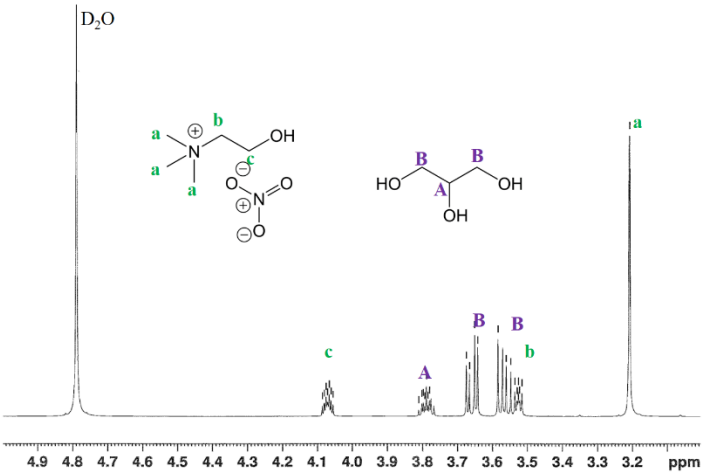

Figure 5. ^{1}H NMR spectrum of neat [Cho][NO_3] – Glycerol

4.3. SPOT PLATE TESTING

Spot-plate testing was performed to qualitatively determine the reactivity of each of the propellants, and therefore used to decide which propellants merit further quantitative reactivity testing. In spot-plate testing a single droplet of propellant is placed on a heated catalyst at atmospheric conditions. Visual evolution of the propellant is documented. A Thermo-Scientific ceramic digital hot plate was used to create the constant temperature heated surface. A single droplet with a volume of approximately 10 µL was placed on the catalytic material via a Hamilton 100 µL micro-syringe. The catalyst materials were platinum, rhenium, and titanium foil. Since this analysis is qualitative, the size of the pieces of foil were chosen arbitrarily to be the same size as the pieces of foil described in Section 5 below. A summary of the important aspects of this qualitative analysis are provided in Table 4, including decomposition onset temperature, time delay between the droplet impacting the catalytic surface and the start of decomposition, duration of time for the decomposition event to occur, and observational reports of the residuals left from the

decomposition event. Results from this study agree well with spot-plate testing of [Emim][$EtSO_4$], HAN, and propellant A from our previous work.[34]

Propellant A decomposed at temperatures as low as 90 ^oC, but the delay from the propellant droplets time of impact to the visual observation of smoke, and the time duration after the initial observation were too great for qualitative analysis. Therefore, the temperature was increased to 150^oC for propellant A, and rapid decomposition events were observed. Platinum foil had the shortest delay and decomposition time; both were approximately one second or less in duration. Rhenium foil had the second fastest decomposition time, but the delay time was approximately 20 seconds. Finally, the titanium tests for propellant A, with both times of interest under 3 seconds, show propellant A is thermally reactive without a catalyst material at temperatures below the decomposition temperature of HAN of 165 ^oC.

Propellants B and C showed some reactivity at 150 ^oC, but had delay and duration times much longer than propellant A. So, the temperature was increased to 200 ^oC. At this temperature propellants B and C showed similar reactivity on platinum and rhenium foils. All the decomposition delays were less than 5 seconds, and all the decomposition times were less than 6 seconds. These times, coupled with the increase in temperature required, show qualitatively that propellants B and C are still reactive, but they are not as chemically reactive as propellant A. This is supported as well by the decomposition times required of this propellant on titanium foil. Both propellant mixtures released smoke within 6 seconds, but it took a minimum of 2 minutes and 45 seconds for the propellant sample to completely decompose. However, even with these long times, it was observed that the violent portion of the decomposition event for the titanium tests for propellants B and C were comparable

in time to those observed for the same propellant mixtures on rhenium and platinum. These violent decomposition event times are less than one second.

Propellants D and E required a temperature of 350ºC to have short delay and duration times. Even at this elevated temperature, the results for propellants D and E were slower than those for propellants B and C. This observation follows the decomposition temperature for each propellant's respective oxidizer. Propellants D and E have AN, which is stable as a solid at room temperature, while HAN is unstable. Furthermore, as their respective enthalpy of formations suggest in Table 1, AN requires more energy to decompose and exothermically react than HAN.

The most significant observation with Propellants D and E, however, comes from the residue left after the decomposition event. For each test performed with these propellants, an almost black, dark brown liquid was left on each foil still bubbling. Each decomposition event was less than 20 seconds, but the time afterwards for the residue to stop bubbling and resemble a solid varied. The residue left from testing with Propellants D and E provided qualitative evidence of incomplete decomposition, while the residue left from testing with propellants A through C provided evidence on the other end of the spectrum. All the tests performed with Propellants B and C have a clear liquid with a slight yellow hint left after each test. A similar observation was made of the propellant left after each test with propellant A. Therefore, due to the residue left after every spot-plate test, and the required temperature in order to achieve a decomposition event, only propellants A, B, and C were chosen for quantitative reactivity analysis.

Table 4. Summary of spot-plate testing results

Propellant	Catalyst	Onset (ºC)	Delay (s)	Duration (s)	Residue
A	Platinum	150	< 1	~ 1	Clear w/ yellow hint liquid
	Rhenium	150	< 20	< 2	Clear w/ yellow hint liquid
	Titanium	150	< 3	< 3	Clear w/ dark yellow hint liquid
B	Platinum	200	< 2	< 5	Clear w/ yellow hint liquid
	Rhenium	200	< 2	< 5	Clear w/ yellow hint liquid
	Titanium	200	< 5	~300	Clear w/ yellow hint liquid
C	Platinum	200	< 5	< 2	Clear w/ yellow hint liquid
	Rhenium	200	< 2	< 6	Clear w/ yellow hint liquid
	Titanium	200	< 6	~ 165	Clear w/ yellow hint liquid
D	Platinum	350	< 3	>20	Brown/black thick liquid
	Rhenium	350	< 3	>20	Brown/black thick liquid
	Titanium	350	< 5	>20	Brown/black thick liquid
E	Platinum	350	< 4	>20	Brown/black thick liquid
	Rhenium	350	< 3	>20	Brown/black thick liquid
	Titanium	350	< 10	>20	Brown/black thick liquid

5. BATCH REACTOR STUDY

Propellants A, B, and C are further analyzed using a batch reactor. The experimental setup is described, followed by results of the temperature evolution of heated samples of these propellants.

5.1. EXPERIMENTAL SETUP

The batch reactor used in this study is similar in function to batch reactors used in previous studies on HAN-based propellants, including propellant A.[26, 34, 42] In a batch reactor, a small sample of propellant is placed on a metallic foil and heated. The temperature of the sample is measured with respect to time. Changes in the temporal evolution of temperature indicate when the propellant begins to decompose and can be

used to determine the onset temperature of decomposition, the temperature rise rate due to self-heating (exothermic decomposition processes) and can aid in selection of the best catalyst materials for the propellant.

5.1.1. General Experimental Setup Description. The batch reactor is shown in Figure 6 (A). A close-up of the sample holder is shown in Figure 6 (B). During a test, propellant is placed in the sample holder, which is then put into the batch reactor chamber. The chamber is evacuated to approximately 100 mTorr, then backfilled with argon. The metallic foil that the propellant is in contact with is heated electrically, and the evolution of the temperature of the metallic foil is measured. The chamber of the batch reactor, Figure 6 (A) Location 1, is approximately 1L in volume, and has four conflat flange ports to provide pressure measurement and control, temperature measurement, power to the catalytic surface, and a port for access. The power supply, a Sorensen DLM 20-30, Figure 6 (A) Location 2, was used to drive current through the metallic foil. A Tektronix DPO 2024 Oscilloscope, Figure 6 (A) Location 3, was used for data triggering and acquisition. The data collected for this experiment were power supply voltage, chamber pressure, and foil temperature. Temperature is measured using a Type-K thermocouple, Figure 6 (A) Location 4 and Figure 6 (B) Location A, connected to an OMEGA CN730 readout, Figure 6 Location 5. Pressure was measured using an OMEGA PXM219 pressure transducer, Figure 6 (A) Location 6, capable of measuring pressures from 0 to 2.5 bar.

The propellant sample used in each test and the metallic foil of interest are contained in the sample holder, which may be viewed in Figure 6 (B) Location B. The sample holder is a 10 mm tall, 5.33 mm inner diameter quartz tube with a 0.54 mm wall

thickness. A 15.3 mm by 25.3 mm piece of Teflon, Figure 6 (B) Location C, with 1.6 mm of thickness contains a 6.4 mm diameter hole to keep the sample holder in place on the metallic foil. A strip of Teflon tape, Figure 6 (B) Location D, was tightly wrapped along the base, both the contacting surface and outer walls, of the sample holder for each test. Due to the quantified high viscosity of [Emim][$EtSO_4$] and the observed high viscosity of [Cho][NO_3], it was determined that the Teflon tape produced an adequate seal for the sample holder. On the lower surface of the rectangular Teflon piece, the metallic foil is placed. The metallic foil and power lead connections, Figure 6 (B) Location E, are kept attached by thin layers of 0.003" thick Kapton tape. The type-K thermocouple used for data acquisition was taped to the bottom face of the Kapton tape directly below the center of the available metallic material for the propellant sample. To provide a voltage across the metallic foil, the two power leads were left bare of insulation, and alligator clips, Figure 6 (B) Location F, were clipped over the Teflon plate, catalytic foil, and power leads to provide an adequate connection. Other connection types were experimented with, including solder and just bare wire connections, but all the other connection options were ruled out due to either material incompatibility or experimental inconsistencies.

Metallic foil is used as the catalyst material in this experiment. In some batch reactor experiments a catalyst powder is used. We choose metallic foil here to better approximate the proposed multi-mode micropropulsion chemical mode, that is, a catalytic microtube. In this case the propellant will be in contact with a monolithic surface of catalyst material as it flows through the tube, not a catalyst powder bed.

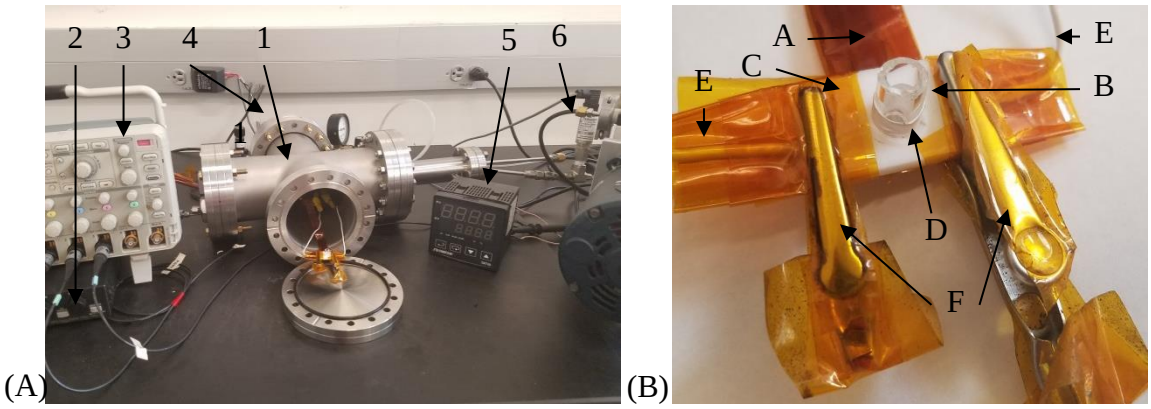

(A) (B)

Figure 6 Experimental Setup for (A) Batch Reactor and (B) Sample Holder

For each test 10 µL of propellant was injected onto the metallic surface in the sample holder via a 100 µL Hamilton micro-syringe. To lower the risk of contamination of the entire volume of propellant available, a sterile, plastic pipette was used to extract a desired amount of propellant for multiple tests, and the syringe was then inserted into the pipette to extract the propellant test sample. The sample holder was then placed inside the batch reactor, all openings were closed, and the system was brought to rough vacuum (~100mTorr), then backfilled to one atmosphere of Argon. The test was started by pressing the power button on the power supply. The oscilloscope then records the data 2 seconds prior to and 18 seconds after the triggering event. Power to the experiment is not turned off until after the 18 second testing window has passed. Three catalyst materials were selected for this experiment: platinum, rhenium, and titanium. Platinum foil was chosen due to it being the material of choice for past microtube thruster experiments,[14-16] rhenium was chosen from previous studies as a possibly good candidate for catalyst materials,[34] and titanium was chosen to provide decomposition events absent of catalytic activity since it is expected to be compatible with HAN-based propellants.[43, 44] The properties required

for this study, along with the desired dimensions of the pieces of foil used in this experiment are provided in Table 5.

Table 5. Used Catalytic Thermal, Electrical, and Dimensional Properties for this Study

Material	ρ [Ω-m]x10^{-7}	κ [W/m-K]	T_m [K]	Length [mm]	Width [mm]	Thickness [mm]
Platinum	1.04	71.6	1968	27	5.5	0.025
Rhenium	1.85	71	3382	25	5.5	0.025
Titanium	4.27	20.8	1868	25	5.5	0.05

5.1.2. Temperature Data Acquisition Description. Temporal evolution of the temperature of the metallic catalyst foil is measured with a type-K thermocouple. The thermocouple voltage output is measured with a digital oscilloscope. The voltage-temperature calibration curve was determined using an OMEGA CN730 calibrated for a Type-K thermocouple. Specifically, a blank foil strip is electrically heated to a set temperature, and the oscilloscope voltage and OMEGA CN730 temperature output are both recorded. A 9th degree polynomial equation was fit to the voltage-temperature data. The OMEGA CN730 has a manufacturer quoted error of 0.1%, and comparing the curve fit to the calibration data shows that the percent error within the temperature range important to this study, between 50^{o}C and 300^{o}C, is less than 5%.

6. EXPERIMENTAL RESULTS AND ANALYSIS

Temperature as a function of time for propellants A, B, and C on platinum, rhenium, and titanium foils are acquired. A common trend between the results is the initial rise in temperature, followed by an abrupt change in slope, as noted on Figure 7A as the decomposition temperature. The abrupt change in slope indicates a change in the heating

rate. To understand these results, it is important to recognize that the sample holder is heated by two main processes: 1) electrical/resistive (subscript E) heating due to the electrical current and 2) heating due to exothermic decomposition of the propellant (self-heating, subscript S). This is illustrated mathematically as equation 1. Equation 2 gives the relationship for electrical heating, where $\dot{Q}$ is the electrical heating rate. Equation 3 gives the relationship for the self-heating rate, which is a function of the heat of reaction and reaction rate of the propellant. Equation 4 is the substitution of equation 2 and 3 into equation 1. As shown in Figure 7A, at early times the sample holder is being heated entirely electrically. At a certain time, a temperature is reached that causes the heating rate to change, we call this the decomposition temperature. At this temperature the sample is now being heated both electrically and by self-heating (exothermic decomposition of propellant).

$$\frac{dT}{dt} = \dot{T}_E + \dot{T}_S \quad \textbf{(1)}$$

$$\dot{T}_E = \frac{\dot{Q}}{\sum N_i C_{p,i}} \quad \textbf{(2)}$$

$$\dot{T}_S = \frac{(-\Delta H_{Rx})(-r_A V)}{\sum N_i C_{p,i}} \quad \textbf{(3)}$$

$$\frac{dT}{dt} = \frac{\dot{Q} + (-\Delta H_{RX})(-r_A V)}{\sum N_i C_{p,i}} \quad \textbf{(4)}$$

We are primarily interested in the decomposition temperature and self-heating rate of the propellants on different catalyst materials. We report the decomposition temperature as the temperature corresponding to the change in slope as shown in Figure 7A. We calculate the self-heating rate by first subtracting the electrical heating rate from the data, and then calculating the slope of the data after the decomposition temperature.

Specifically, we fit a two-term, exponential curve of the form given in equation 5 between time zero and the time corresponding to the decomposition temperature (Figure 7A). We then subtract this curve from the data, thereby removing the temperature increase due to electrical heating, such that only the temperature change due to self-heating remains. We then fit a line to the temperature data directly after the decomposition temperature (Figure 7B). We report the slope of this line as the self-heating rate.

$$T(t) = a * e^{bt} + c * e^{dt} \quad \textbf{(5)}$$

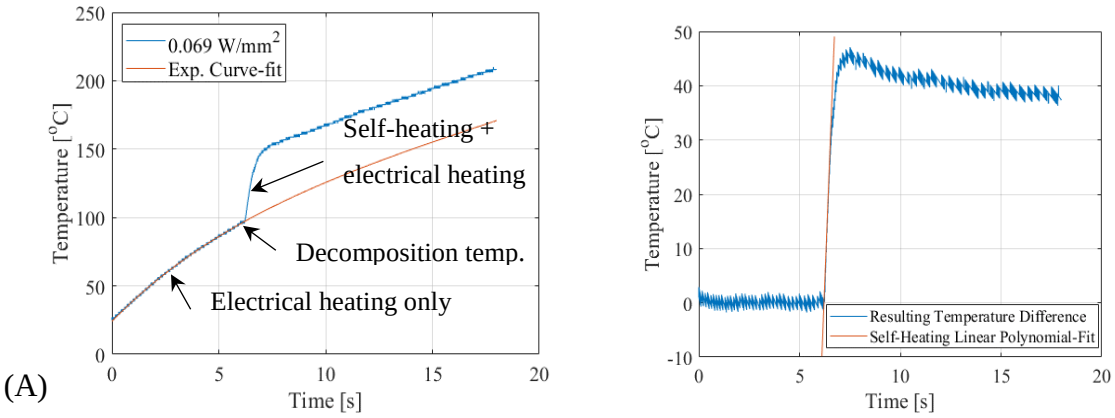

(A)

Figure 7. Example of data analysis showing (A) curve fit to the electrical-heating rate and (B) linear fit to the self-heating rate

Temperature as a function of time for propellants A, B, and C on platinum, rhenium, and titanium foils are shown in Figure 8, Figure 9, and Figure 10, respectively. These data are analyzed as described above and the decomposition temperature and self-heating rate

are summarized in Table 6. The heating rate per unit area applied to the metallic foils is calculated using equation 6.

$$\dot{Q}'' = I^2 \left(\frac{L}{k * w * t * \pi * r_{holder}^2} \right) \quad \textbf{(6)}$$

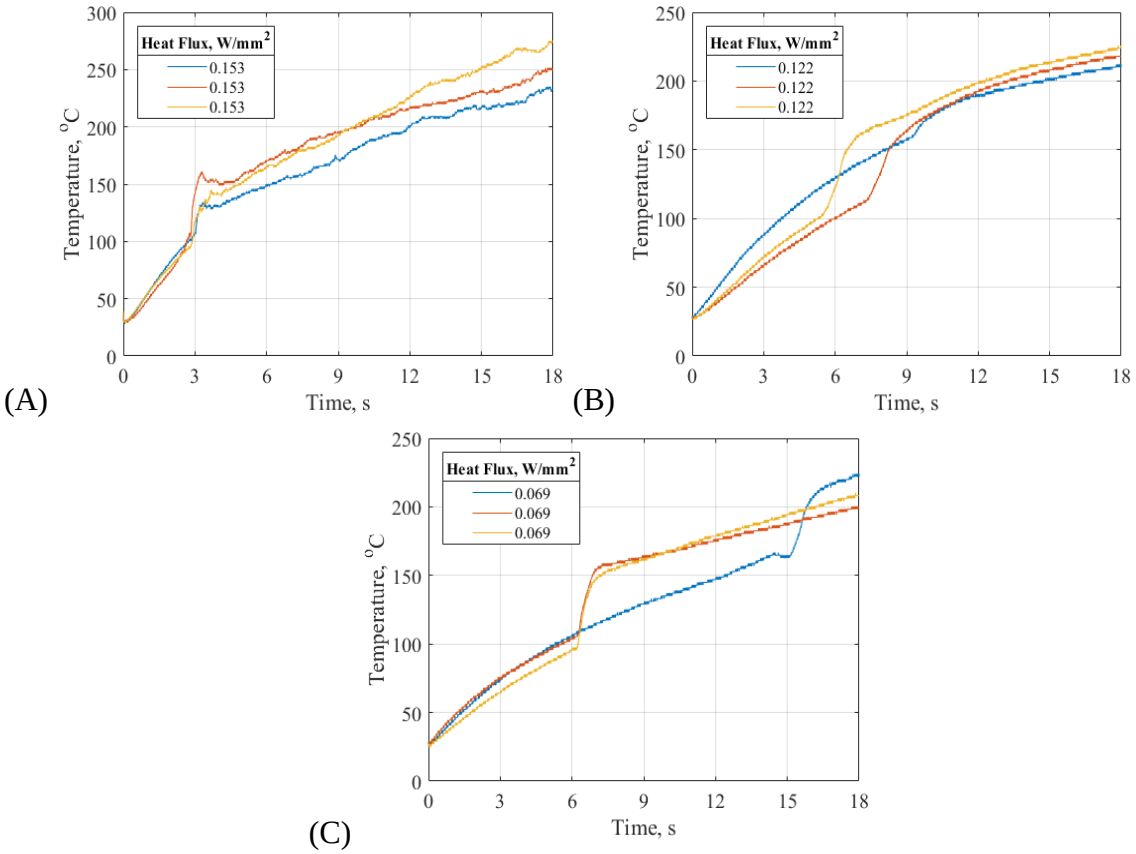

Figure 8. Propellant A decomposition on (A) platinum, (B) rhenium, and (C) titanium foils

Results for the decomposition of propellant A are presented in Figure 8. Data for platinum is shown in Figure 8A. The decomposition temperatures for these tests are 107°C, 108°C, and 94°C respectively. The average decomposition temperature is 18°C, 21%, higher than the previously determined results. The self-heating rates for these tests are 242,

272, and 276^{o}C/sec respectively. These are approximately 100 ^{o}C/sec slower determined self-heating rates from previous experimentation. This difference in self-heating rates and similarity in decomposition temperatures could be caused by the difference in procedures for determining the self-heating rate. In the previous study, the self-heating rate was determined from the original data set of temperature versus time, while this analysis was performed by removing the electrical heating rate via the procedure described above. The decomposition temperature increases, and the self-heating rates decrease for both rhenium and titanium test sets when compared to the platinum foil results, as shown in Figure 8B and Figure 8C. However, the determined self-heating rate for titanium was faster than rhenium, which contradicts the previously determined self-heating rates for this propellant.

Results for the decomposition of propellant B are presented in Figure 9. The decomposition temperatures for each foil have increased significantly compared to the propellant A results. Specifically, propellant B has decomposition temperatures approximately 90 to 100^{o}C higher than propellant A for platinum, 5 to 50^{o}C higher for rhenium, and 5 to 90^{o}C higher for titanium. The decomposition temperature for each test was more consistent for this propellant when compared to the decomposition temperatures found for propellant A. The determined-self heating rates significantly decreased for all three foils, especially platinum. The self-heating rate for this propellant on platinum foil has the smallest self-heating rate, and both rhenium and titanium tests have average self-heating rates close to 40^{o}C/sec. This is a significant difference from the results for propellant A and will be discussed further in the discussion section.

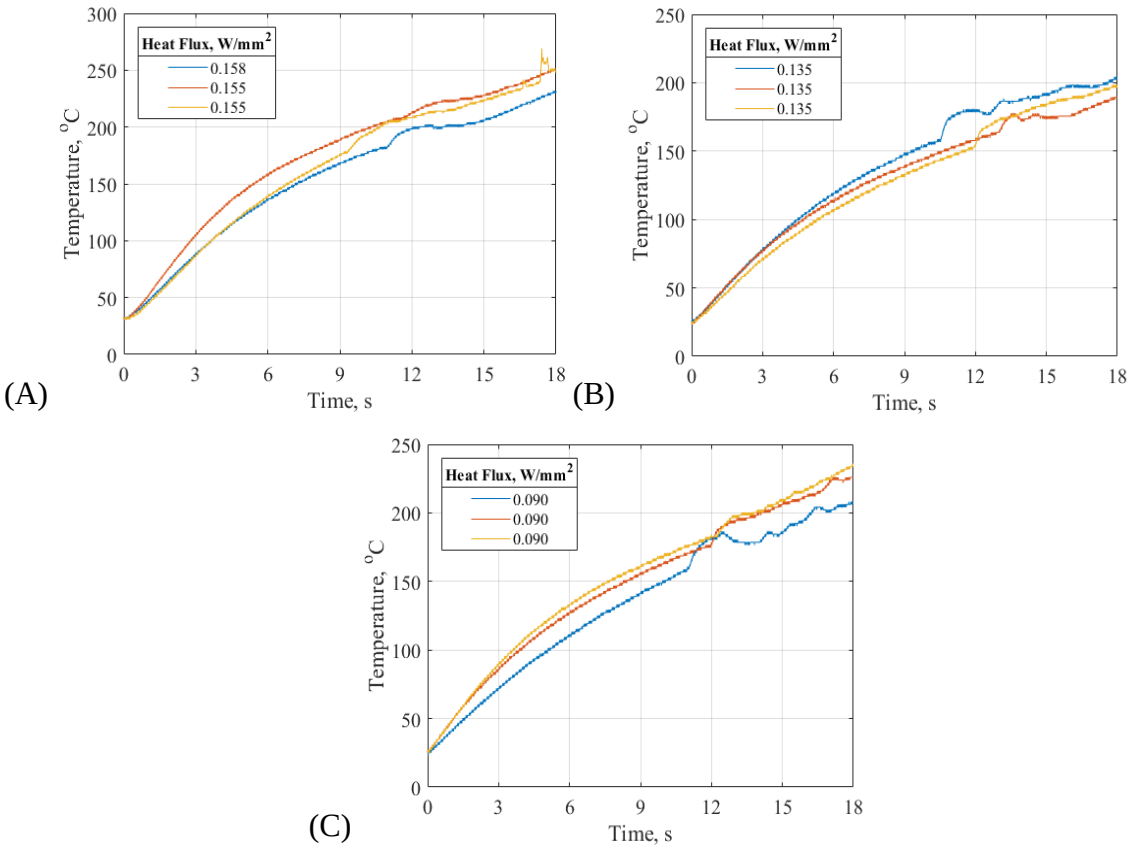

Figure 9. Propellant B decomposition on (A) platinum, (B) rhenium, and (C) titanium foils

Results for the decomposition of propellant C are presented in Figure 10. The decomposition temperature was determined for each of the tests for this propellant, but a self-heating rate for an exothermic reaction was determined for only two of these tests. Four of the tests performed with propellant C had decreases in temperature after the determined decomposition temperatures, while the fifth test had a constant increase in temperature after the decomposition temperature. The decomposition temperatures on platinum foil were 181ºC and 168ºC with a determined self-heating rate of 8ºC/s for the first decomposition temperature. Testing on rhenium foil produced two tests with no self-heating rates related to an exothermic reaction. These tests had decomposition

temperatures of 219ºC and 203ºC. Titanium had the largest variance in decomposition temperatures with the lowest observed temperature at 178ºC, and the highest at 247ºC. Titanium had the only other measurable self-heating rate of 37ºC/s. This decomposition rate is slightly slower, but comparable to the calculated self-heating rates for Propellant B. These results, along with possible explanations for this behavior are discussed in the following section.

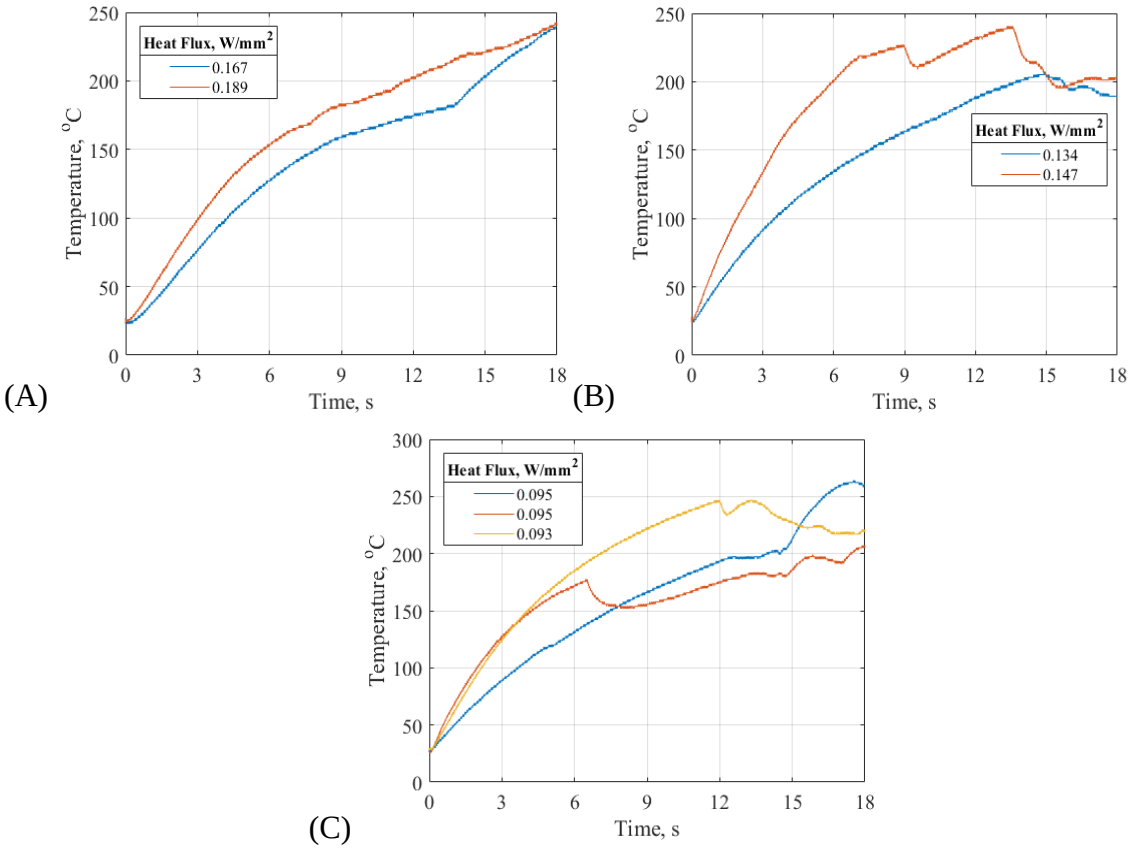

Figure 10. Propellant C decomposition on (A) platinum, (B) rhenium, and (C) titanium foils

Table 6. Heat flux, decomposition temperature, and self-heating rate of propellants A, B, and C on different catalyst foils

	Material	Platinum			Rhenium			Titanium		
Propellant	**Test #**	**1**	**2**	**3**	**1**	**2**	**3**	**1**	**2**	**3**
A	$\dot{Q}$" (W/mm^2)	0.153	0.153	0.153	0.122	0.122	0.122	0.069	0.069	0.069
	T_{decomp}(°C)	108	107	94	159	113	104	165	105	96
	$\dot{T}_S$ (°C/s)	243	272	276	28	32	30	73	95	95
B	$\dot{Q}$" (W/mm^2)	0.158	0.155	0.146	0.135	0.135	0.135	0.090	0.090	0.090
	T_{decomp}(°C)	181	208	190	157	164	153	160	175	183
	$\dot{T}_S$ (°C/s)	25	6	15	45	36	43	40	41	40
C	$\dot{Q}$" (W/mm^2)	0.167	0.189		0.134	0.147		0.095	0.095	0.095
	T_{decomp}(°C)	181	168		219	203		197	178	247
	$\dot{T}_S$ (°C/s)	8	-		-	-		37	-	-

7. DISCUSSION

This section discusses the results presented in the previous section.

7.1. PROPELLANTS COMPARISON

The most significant results from this analysis are with respect to the platinum foil. The novel propellant mixtures have over 200°C/s smaller self-heating rates on platinum foil when compared with the previously studied binary mixture, propellant A, and there is at least a 75°C decomposition temperature increase. Also, when compared with [Cho][NO_3] – glycerol testing on the other foils of interest, the platinum self-heating rates are at least 10°C/s slower and the decomposition temperatures are, on average, at least 20°C higher for propellant B. This is the exact opposite relation from propellant A. Platinum foil is a known catalyst for oxygen and hydrogen reactions, which is a reason this foil was

chosen for this experiment and similar past experiments. It is unknown why this difference in performance arises, but it could imply that the difference in the reaction processes of the two propellants is significant enough to cause the shown decrease in platinum's catalyst effects on [Cho][NO_3] – glycerol monopropellant mixtures. Similarly, the titanium results for propellants B and C have approximately 50^{o}C/s slower self-heating rates when compared to propellant A, and an average 50^{o}C higher decomposition onset temperature. The qualitative spot-plate tests support these changes as well because the onset temperature had to be increased by 50^{o}C, and the time durations of decomposition increased by at least one second.

The rhenium results, however, do not follow these trends. The average decomposition temperature does increase from propellant A to B and C by at least 33^{o}C, but the self-heating rate increased from an average of 30^{o}C/s to 41^{o}C/s as well. This is the opposite trend of the two other catalytic materials. This could mean that the [Cho][NO_3] – glycerol reacts more with rhenium than platinum and titanium foils. Overall, however, the results indicate [Emim][$EtSO_4$]-HAN with platinum catalyst is still the most promising as a multi-mode micropropulsion propellant and catalyst material combination.

7.2. EVIDENCE OF ENDOTHERMIC REACTIONS

The [Cho][NO_3] – glycerol propellant, particularly propellant C, shows evidence of endothermic reactions. As noted above in Figure 10, after the decomposition temperature the temperature decreases in some tests of propellant C. Similar results were observed for some propellant B tests, but a decrease in temperature occurred more often for propellant C tests. This leads us to believe that [Cho][NO_3] – glycerol is the main cause of the

temperature decrease since it has a higher concentration in propellant C. These results may be indicative of an endothermic reaction. [Cho][NO_3] – glycerol decomposition process may contain, at least initially, endothermic reaction steps. If this hypothesis is correct, then in the experiments a temperature decrease would be measured if the heat absorption of the propellant (endothermic) is greater than the heat addition due to electrical heating. Therefore, increasing the electrical heating rate should eliminate or reduce the decreasing temperature trend. This is indeed what we find in Figure 11. An initial study of this hypothesis was performed with propellant B on platinum foil. The current applied between the two tests was increased by 1A, and the increase in heat flux from the electrical current increase results in a significant change in the temperature temporal profile, i.e., the decomposition characteristics, which is shown in Figure 11. These results show a significant drop in the decomposition temperature, and a difference between the type of reaction, endothermic to exothermic, as the heat flux applied to the propellant sample increases.

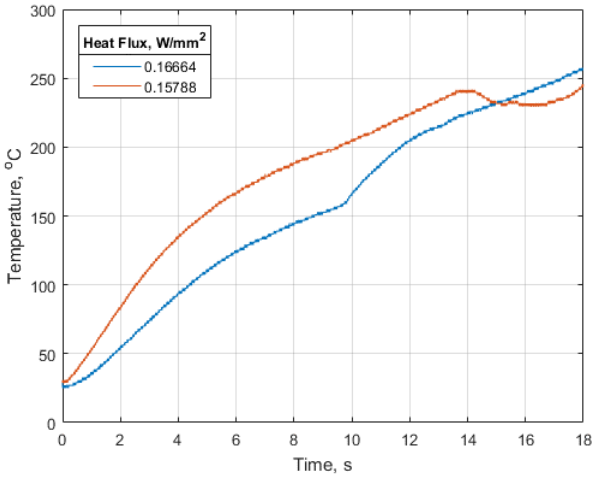

Figure 11. Temperature vs. time for different applied heat fluxes for propellant B on platinum foil

This type of reaction follows results from a well-developed monopropellant developed by the Air Force, AFM315-E. However, the higher heat fluxes required to produce the quantifiable exothermic reactions required for further analysis, including Arrhenius reaction rate coefficients, have a high probability of overheating the Teflon components of the experimental setup, and are not studied within this initial analysis.

8. CONCLUSION

Five propellants were experimentally characterized in this work with envisioned application as multi-mode micropropulsion propellants. Four of which (B, C, D, E) were new propellants with a novel ionic liquid fuel, [Cho][NO_3] – glycerol. The fifth propellant (A) is our previously investigated and promising propellant that is a mixture of [Emim][$EtSO_4$]-HAN. Propellants D and E used AN oxidizer with the new fuel, but required high temperatures to initiate decomposition and are unlikely to be viable for the application. Propellants B and C used HAN oxidizer with the new fuel. Propellants B and C have significantly lower self-heating rates, approximately 240 $^oC/s$ lower, than the self-heating rate of propellant A at similar heat flux values. The heating rates for propellant B on rhenium and titanium foils were both determined to be approximately 40 $^oC/s$, and the decomposition temperatures were approximately 158 ^oC and 173 ^oC respectively. These decomposition temperatures are both in close proximity to the decomposition of HAN at 165 ^oC, but are higher than the decomposition temperatures obtained for propellant A in this and previous studies. When heated on rhenium and titanium foils, propellant C experienced endothermic decomposition events, and an unquantifiable exothermic decomposition event on platinum foil. Therefore, further study of this propellant mixture

with higher heat fluxes into the propellant sample are required to obtain quantifiable exothermic decomposition events.

Theoretically the novel ionic liquid binary mixtures, propellants B and C, can perform better than propellant A with respect to I_{sp}, approximately 280 versus 250 seconds, while operating at lower or similar combustion temperatures, 1300K versus 1900K. Therefore, design studies taking power requirements, total mass, available momentum change, and performance characteristics are required to determine which monopropellant mixture is ideal for a multi-mode micropropulsion system. However, with this initial study, the results indicate [Emim][$EtSO_4$]-HAN with platinum catalyst is still the most promising as a multi-mode micropropulsion propellant and catalyst material combination.

ACKNOWLEDGMENTS

Partial support for this work was provided by the University of Missouri System through the FastTrack program, Air Force Nanosatellite 9 program, and NASA Undergraduate Student Instrument Project. The authors would also like to thank the researchers of the Aerospace Plasma Laboratory for their assistance throughout this experiment, and providing insightful information. Finally, the authors thank the technicians within the department machine shop for their assistance in the manufacturing process of this experiment.

REFERENCE

[1] T. Rexius and M. Holmes, "Mission Capability Gains from Multi-Mode Propulsion Thrust Profile Variations for a Plane Change Maneuver," *AIAA Modeling and Simulation Technologies Conference*, American Institute of Aeronautics and Astronautics, 2011.
doi:10.2514/6.2011-6431

[2] J. Hass and M. Holmes, *Multi-Mode Propulsion System for the Expansion of Small Satellite Capabilities*, 2010.

[3] B. R. Donius and J. L. Rovey, "Ionic Liquid Dual-Mode Spacecraft Propulsion Assessment," *Journal of Spacecraft and Rockets*, Vol. 48, No. 1, pp. 110-123, 2011.
doi: 10.2514/1.49959

[4] B. Donius and J. Rovey, "Analysis and Prediction of Dual-Mode Chemical and Electric Ionic Liquid Propulsion Performance," *48th AIAA Aerospace Sciences Meeting Including the New Horizons Forum and Aerospace Exposition*, American Institute of Aeronautics and Astronautics, 2010.
doi:10.2514/6.2010-1328

[5] S. P. Berg and J. L. Rovey, "Assessment of Multimode Spacecraft Micropropulsion Systems," *Journal of Spacecraft and Rockets*, Vol. 54, No. 3, pp. 592-601, 2017.
doi: 10.2514/1.A33649

[6] S. P. Berg and J. L. Rovey, "Assessment of High-Power Electric Multi-Mode Spacecraft Propulsion Concepts," *33rd Internation Electric Propulsion Conference*, 2013.

[7] C. A. Kluever, "Spacecraft Optimization with Combined Chemical-Electric Propulsion," *Journal of Spacecraft and Rockets*, Vol. 32, No. 2, pp. 378-379, 1995.
doi: 10.2514/3.26623

[8] C. A. Kluever, "Optimal Geostationary Orbit Transfers Using Onboard Chemical-Electric Propulsion," *Journal of Spacecraft and Rockets*, Vol. 49, No. 6, pp. 1174-1182, 2012.
doi: 10.2514/1.A32213

[9] D. Y. Oh, T. Randolph, S. Kimbrel and M. Martinez-Sanchez, "End-to-End Optimization of Chemical-Electric Orbit-Raising Missions," *Journal of Spacecraft and Rockets*, Vol. 41, No. 5, pp. 831-839, 2004.
doi: 10.2514/1.13096

[10] S. R. Oleson, R. M. Myers, C. A. Kluever, J. P. Riehl and F. M. Curran, "Advanced Propulsion for Geostationary Orbit Insertion and North-South Station Keeping," *Journal of Spacecraft and Rockets,* Vol. 34, No. 1, pp. 22-28, 1997.
doi: 10.2514/2.3187

[11] S. P. Berg and J. L. Rovey, "Assessment of Imidazole-Based Ionic Liquids as Dual-Mode Spacecraft Propellants," *Journal of Propulsion and Power,* Vol. 29, No. 2, pp. 339-351, 2013.
doi: 10.2514/1.B34341

[12] Y.-h. Chiu and R. A. Dressler, *Ionic Liquids for Space Propulsion,* ACS Publications, Washington, D. C., 2007.

[13] M. Gamero-Castaño, "Characterization of a Six-Emitter Colloid Thruster Using a Torsional Balance," *Journal of Propulsion and Power*, Vol. 20, No. 4, pp. 736-741, 2004.
10.2514/1.2470

[14] G. A. Boyarko, C.-J. Sung and S. J. Schneider, "Catalyzed Combustion of Hydrogen–Oxygen in Platinum Tubes for Micro-Propulsion Applications," *Proceedings of the Combustion Institute*, Vol. 30, No. 2, pp. 2481-2488, 2005.
https://doi.org/10.1016/j.proci.2004.08.203

[15] C. A. Mento, C.-J. Sung, A. F. Ibarreta and S. J. Schneider, "Catalyzed Ignition of Using Methane/Hydrogen Fuel in a Microtube for Microthruster Applications," *Journal of Propulsion and Power,* Vol. 25, No. 6, pp. 1203-1210, 2009.
doi: 10.2514/6.2006-4871

[16] S. J. Volchko, C.-J. Sung, Y. Huang and S. J. Schneider, "Catalytic Combustion of Rich Methane/Oxygen Mixtures for Micropropulsion Applications," *Journal of Propulsion and Power,* Vol. 22, No. 3, pp. 684-693, 2006.
doi: 10.2514/1.19809

[17] M. S. Alexander, J. Stark, K. L. Smith, B. Stevens and B. Kent, "Electrospray Performance of Microfabricated Colloid Thruster Arrays," *Journal of Propulsion and Power,* Vol. 22, No. 3, pp. 620-627, 2006.
doi: 10.2514/1.15190

[18] S. P. Berg and J. L. Rovey, "Design and Development of a Multi-Mode Monopropellant Electrospray Mircropropulsion System," 2016.

[19] P. S. George and B. Oscar, *Rocket Propulsion Elements*, Wiley, OSCAR BIBLARZ, 2001.

[20] D. Amariei, L. Courthéoux, S. Rossignol, Y. Batonneau, C. Kappenstein, M. Ford and N. Pillet, "Influence of Fuel on Thermal and Catalytic Decompositions of Ionic Liquid Monopropellants," *41st AIAA/ASME/SAE/ASEE Joint Propulsion Conference & Exhibit*, American Institute of Aeronautics and Astronautics, 2005. doi:10.2514/6.2005-3980

[21] K. Anflo and T.-A. Grönland, "Towards Green Propulsion for Spacecraft with Adn-Based Monopropellants," *38th AIAA/ASME/SAE/ASEE Joint Propulsion Conference & Exhibit*, American Institute of Aeronautics and Astronautics, 2002. doi:10.2514/6.2002-3847

[22] K. Anflo, S. Persson, P. Thormahlen, G. Bergman and T. Hasanof, "Flight Demonstration of an Adn-Based Propulsion System on the Prisma Satellite," *42nd AIAA/ASME/SAE/ASEE Joint Propulsion Conference & Exhibit*, American Institute of Aeronautics and Astronautics, 2006. doi:10.2514/6.2006-5212

[23] B. Slettenhaar, J. Zevenbergen, H. Pasman, A. Maree and J. Moerel, "Study on Catalytic Ignition of Hnf Based Non Toxic Monopropellants," *39th AIAA/ASME/SAE/ASEE Joint Propulsion Conference and Exhibit*, AIAA Paper 2003-4920, 2003. doi: 10.2514/6.2003-4920

[24] C. H. McLean, "Green Propellant Infusion Mission Program Development and Technology Maturation," *50th AIAA/ASME/SAE/ASEE Joint Propulsion Conference*, American Institute of Aeronautics and Astronautics, 2014. doi:10.2514/6.2014-3481

[25] K. Anflo and R. Möllerberg, "Flight Demonstration of New Thruster and Green Propellant Technology on the Prisma Satellite," *Acta Astronautica*, Vol. 65, No. 9, pp. 1238-1249, 2009. https://doi.org/10.1016/j.actaastro.2009.03.056

[26] S. P. Berg and J. L. Rovey, "Decomposition of Monopropellant Blends of Hydroxylammonium Nitrate and Imidazole-Based Ionic Liquid Fuels," *Journal of Propulsion and Power*, Vol. 29, No. 1, pp. 125-135, 2012. doi: 10.2514/1.B34584

[27] S. P. Berg, J. Rovey, B. Prince, S. Miller and R. Bemish, "Electrospray of an Energetic Ionic Liquid Monopropellant for Multi-Mode Micropropulsion Applications," *51st AIAA/SAE/ASEE Joint Propulsion Conference*, American Institute of Aeronautics and Astronautics, 2015. doi:10.2514/6.2015-4011

[28] S. P. Berg and J. Rovey, "Decomposition of a Double Salt Ionic Liquid Monopropellant in a Microtube for Multi-Mode Micropropulsion Applications," *53rd AIAA/SAE/ASEE Joint Propulsion Conference*, American Institute of Aeronautics and Astronautics, 2017.
doi:10.2514/6.2017-4755

[29] A. Mundahl, S. P. Berg and J. Rovey, "Linear Burn Rates of Monopropellants for Multi-Mode Micropropulsion," *52nd AIAA/SAE/ASEE Joint Propulsion Conference*, American Institute of Aeronautics and Astronautics, 2016.
doi:10.2514/6.2016-4579

[30] Y.-P. Chang, "Combustion Behavior of Han-Based Liquid Propellants," Mechanical Engineering, The Pennsylvania State University, 2002.

[31] T. Katsumi, K. Hori, R. Matsuda and T. Inoue, "Combustion Wave Structure of Hydroxylammonium Nitrate Aqueous Solutions," *46th AIAA/ASME/SAE/ASEE Joint Propulsion Conference & Exhibit*, American Institute of Aeronautics and Astronautics, 2010.
doi:10.2514/6.2010-6900

[32] K. W. McCown, G. Homan-Cruz and E. L. Petersen, "Effects of Nano-Scale Additives and Methanol on the Linear Burning Rates of Aqueous Han Solutions," *50th AIAA/ASME/SAE/ASEE Joint Propulsion Conference*, American Institute of Aeronautics and Astronautics, 2014.
doi:10.2514/6.2014-3566

[33] J. Hass and M. Holmes, *Multi-Mode Propulsion System for the Expansion of Small Satellite Capabilities*, NATO, 2010.

[34] S. P. Berg and J. Rovey, "Decomposition of a Double Salt Ionic Liquid Monopropellant on Heated Metallic Surfaces," *52nd AIAA/SAE/ASEE Joint Propulsion Conference*, American Institute of Aeronautics and Astronautics, 2016.
doi:10.2514/6.2016-4578

[35] Z.-H. Zhang, Z.-C. Tan, L.-X. Sun, Y. Jia-Zhen, X.-C. Lv and Q. Shi, "Thermodynamic Investigation of Room Temperature Ionic Liquid: The Heat Capacity and Standard Enthalpy of Formation of Emies," *Thermochimica Acta*, Vol. 447, No. 2, pp. 141-146, 2006.

[36] P. S. o. A. a. Astronautics, *Propulsion Web Page*, Purdue School of Aeronautics and Astronautics,

[37] S. Berg and J. Rovey, *Dual-Mode Propellant Properties and Performance Analysis of Energetic Ionic Liquids*, 2012.

[38] N. Klein, "Liquid Propellant for Usin in Guns - a Review," Rept. BRL-TR-2641, 1985.

[39] C. P. I. A. C. MD., *Cpia/M5 Liquid Propellant Engine Manual October 1992 Supplement (Unit No. 228),* Defense Technical Information Center, 1992.

[40] K. Anflo, S. Persson, P. Thormahlen, G. Bergman and T. Hasanof, *Flight Demonstration of an Adn-Based Propulsion System on the Prisma Satellite,* 2006.

[41] B. G. Pfrommer, F. Mauri and S. G. Louie, "Nmr Chemical Shifts of Ice and Liquid Water: The Effects of Condensation," *Journal of the American Chemical Society*, Vol. 122, No. 1, pp. 123-129, 2000.

[42] R. Eloirdi, S. Rossignol, C. Kappenstein, D. Duprez and N. Pillet, "Design and Use of a Batch Reactor for Catalytic Decomposition of Propellants," *Journal of Propulsion and Power*, Vol. 19, No. 2, pp. 213-219, 2003.

[43] E. W. Schmidt, *Hydroxylammonium Nitrate Compatibility Tests with Various Materials-a Liquid Propellant Study,* DTIC Document, 1990.

[44] C. H. McLean, *Green Propellant Infusion Mission Program Development and Technology Maturation,* 2014.

II. LINEAR BURN RATE OF MONOPROPELLANT FOR MULTI-MODE MICROPROPULSION

Alex J. Mundahl[8]

Missouri University of Science and Technology, Rolla, Missouri 65409, United States of America

Steven P. Berg[9] and Joshua L. Rovey[10]

University of Illinois at Urbana-Champaign, Urbana, Illinois 61801, United States of America

ABSTRACT

Multi-mode micropropulsion is a potential game-changing technology enabling rapidly composable small satellites with unprecedented mission flexibility. Maximum mission flexibility requires propellant that is shared between the chemical and electric propulsion systems. Previous research has identified a promising monopropellant that is both readily catalytically exothermically decomposed (chemical mode) and electrosprayable (electric mode). In this work the linear burn rate of this monopropellant is determined and used to aid design of a microtube catalytic chemical thruster. Experiments with a pressurized fixed volume reactor are used to determine the linear burn rate.

---

[8] Graduate Research Assistant, Aerospace Plasma Laboratory, Mechanical and Aerospace Engineering, 160 Toomey Hall, 400 W. 13th Street, Student Member AIAA.

[9] Intelligence Community Postdoctoral Fellow, Department of Aerospace Engineering, Talbot Laboratory, 104 South Wright Street, Senior Member AIAA.

[10] Associate Professor of Aerospace Engineering, Department of Aerospace Engineering, 317 Talbot Laboratory, 104 South Wright Street, Associate Fellow AIAA.

Benchmark experiments use a 13-molar mixture of hydroxylammonium nitrate and water and show agreement to within 5% of literature data. The multi-mode monopropellant is a double-salt ionic liquid consisting of 41% 1-ethyl-3-methylimidazolium ethyl sulfate and 59% hydroxylammonium nitrate by mass. At the design pressure of 1.5 MPa the linear burn rate of this propellant is 26.4 ± 2.5 mm/s. Based on this result, the minimum flow rate required for a microtube with a 0.1 mm inner diameter within the pressure range tested is between 0.12 and 0.35 mg/s.

NOMENCLATURE

r_b = linear burn rate [mm/s]

D_c = Diameter of propellant container [cm]

D_t = Diameter of microtube [cm]

m_p = mass of propellant used [g]

$\dot{m}_p$ = mass flow rate of propellant [mg/s]

Δx = change in position [mm]

Δt = change in time [s]

ρ_p = density of propellant used [g/cm^3]

1. INTRODUCTION

Multi-mode propulsion is the use of two or more integrated, yet fundamentally different propulsive modes on a single spacecraft. Recently proposed systems make use of a high-specific impulse, usually electric mode, and a high-thrust, usually chemical mode. This can be beneficial in two primary ways: an increase in mission flexibility,[1-3, 5, 6]

and the potential to design a more efficient orbit[8-10, 45]. An increase in mission flexibility is achieved due to the availability of the two differing propulsive maneuvers to the mission designer at any point during the mission. This allows for drastic changes to the mission thrust profile at virtually any time before or even after launch without the need to integrate an entirely new propulsion system. Additionally, it has been shown that under certain mission scenarios it is beneficial in terms of spacecraft mass savings, or deliverable payload, to utilize separate high-specific impulse and high-thrust propulsion systems even in hybrid propulsion systems [9, 45, 46]. However, even greater mass savings can be realized by using a shared propellant and/or hardware, even if the thrusters perform lower than state-of-the-art in either mode [3, 11]. In order to realize the full potential of a multi-mode propulsion system, it is necessary to utilize one shared propellant for both modes; this allows for a large range of possible maneuvers while still allowing for all propellant to be consumed regardless of the specific choice or order of maneuvers [6]. Two propellants have been developed that can function as both a chemical monopropellant and an electrospray propellant [11]. These monopropellants have been previously synthesized and assessed for thermal and catalytic decomposition within a microreactor,[26] and for performance in an electrospray emitter [27]. One of the monopropellant combinations, a mixture of 1-ethyl-3-methylimidazolium ethyl sulfate ([Emim][$EtSO_4$]) and hydroxylammonium nitrate (HAN), has also been further analyzed to determine its decomposition characteristics on relevant catalytic surfaces [26, 34, 47]. This paper further studies the characteristics of the [Emim][$EtSO_4$]-HAN monopropellant by determining the linear burn rate of this propellant at pressures relevant to typical monopropellant thruster operation [34, 48].

Recent efforts in developing propellants for space vehicles have focused on finding a high-performance, low-toxicity propellant replacement for traditional, but highly toxic options. Hydrazine has been chosen for use in gas generators and spacecraft monopropellant thrusters due to its storability and favorable decomposition characteristics that provide relatively high performance [19]. However, hydrazine is difficult from a handling perspective since it is highly toxic. A large amount of the research toward a hydrazine replacement is focused on energetic ionic liquids. An energetic ionic liquid is a molten salt with an energetic functional group capable of rapid exothermic decomposition. Energetic salts that have been studied for such purposes include ammonium dinitramide (ADN), hydrazinium nitroformate (HNF), and hydroxylammonium nitrate (HAN) [19-23]. Typically, these salts are mixed with compatible fuels to improve the performance characteristics of the propellant. However, the high combustion temperatures for these energetic monopropellants have been the main limitation in their practical use in spacecraft thrusters, but recent research in thermal management and materials have mitigated some issues, and multiple flight tests are scheduled, or have already been conducted [12, 24, 25]. These propellants perform well in chemical thrusters, but they are fundamentally unable to perform as an electrospray propellant due to their water content or other volatile component. To overcome this, the previously described monopropellants were developed, synthesized, and shown to be capable of high performance in an electrospray thruster [11, 26].

Small spacecraft have seen a growth in popularity, specifically microsatellites (10-100 kg) and nanosatellites (1-10 kg), including the subset of CubeSats. Many different types of thrusters have been proposed to meet the stringent mass and volume requirements

placed on spacecraft of this type. Electrospray propulsion systems are good options for micropropulsion, and have been selected for such applications [12, 13]. Many different chemical propulsion systems have also been proposed, including the chemical microtube [14-16]. This propulsion system utilizes a heated tube with a typical diameter of 1 mm or less and may also have a catalytic surface material. Additionally, capillary type emitters used for an electrospray propulsion system can be roughly the same diameter tube, and there is therefore no fundamental reason why this geometry could not be shared within a multi-mode propulsive system [17, 49].

The linear burn rate of the propellant used at the thruster anticipated operating pressures is a useful parameter in the design of the system, both for thruster operation and flashback prevention. The linear burn rate has been studied previously for monopropellants, including HAN-based monopropellants [30-32]. This paper presents results on the experimental determination and assessment of the linear burn rate characteristics of the [Emim][$EtSO_4$]-HAN propellant at various pressures using a pressurized strand burner setup. These measurements, taken together, can be used to aid in the design and optimization of a catalytic microtube thruster. Section 2 describes the setup of the experiment, Section 3 presents the results of the experiment, Section 4 discusses the results including relevant development or selection of microtube thruster parameters, and Section 5 presents the conclusions of this study.

2. EXPERIMENTAL SETUP

The pressurized linear burn rate studies performed here are similar to those described in previous studies utilizing HAN-based propellants and nitromethane [50, 51].

In a pressurized linear burn rate experiment a sample of propellant is ignited and combusts within a known sealed volume. Pressure within the volume is measured as a function of time with the propellant burn time determined based on discontinuities within the pressure profile corresponding to the initiation and extinguishment of combustion. Using the measured burn time, known mass of propellant, and known geometry of the propellant sample holder, it is possible to calculate the linear burn rate of the propellant.

The full experimental setup is shown in Figure 1a, and Figure 1b shows the propellant sample holder in more detail. The propellant sample holder is a 5.9-mm-internal-diameter, 45 mm tall quartz tube. It was sized to allow for roughly 1 ml of propellant to be used for each test, and is at location A in Figure 1b. The propellant holder is epoxied on the outer edge to a quartz cylinder. For each test, two pieces of equal length 30-gauge nickel-chromium (nichrome) wire were twisted together and soldered to the electrical leads within the propellant holder stand, and are shown at location B in Figure 1b. The nichrome wires are then bent and submerged within the propellant no more than 5% of the total height of the internal volume available within the propellant holder (~2.25mm). An illustration of this is shown in Figure 1c. Two Solid Sealing Technology 0.05 in diameter copper feedthroughs served as the electrical feedthroughs for the two wires providing electrical power to ignite the propellant, and is at locations 1 and C in Figure 1a and Figure 1b respectively. Propellant is ignited by applying current through, and thus resistively heating, the nickel-chromium wire. The propellant holder stand, shown at location 2 in Figure 1a, attaches to the top flange of the pressure vessel via four threaded rods. The top flange, location 3 in Figure 1a, connects to the stainless-steel pressure vessel, location 4 in Figure 1a, with an approximate volume of 2L. This additional volume acts to minimize the change

in pressure within the setup as the propellant burns. Also connected to the top flange of the pressure vessel is an Omega PX309-300A5V pressure transducer, location 5 in Figure 1a, with an absolute pressure range of 0 to 300 psia. This transducer monitors the pressure versus time within the volume. The 3-way ball hand valve, location 6 in Figure 1a, is used to vent the system following a completed test. The hand valve opens the volume to the laboratory exhaust system, location 7 in Figure 1a. The other gas feedthrough is used to evacuate the setup with a mechanical vacuum pump, location 8 in Figure 1a, or repressurize the evacuated system with inert argon, location 9 in Figure 1a, to the desired test pressure.

Benchmark tests using 13M HAN-water are conducted, followed by tests using the [Emim][EtSO4]-HAN monopropellant. The monopropellant has a mixture ratio of 41% [Emim][EtSO4] to 59% HAN by mass because this is the formulation envisioned for use within a multi-mode propulsion system and the focus of the previous research [5, 6, 11, 26, 27, 48]. The process for synthesizing this propellant is described in detail within previous studies [5, 26, 47]. The 13M HAN-water solution was prepared by drying 24% by wt. HAN-water solution until solid HAN crystals formed, then adding distilled water to the solid HAN for the final solution. Relevant propellant characteristics are given in Table 1.

Table 1. Propellant Characteristics

Propellant Tested	ρ_p	Mass HAN [%]	Mass Other [%]
HAN-Water	1.57 [29, 47]	80	20
[Emim][$EtSO_4$]-HAN	1.53[29, 47]	59	41

(A).

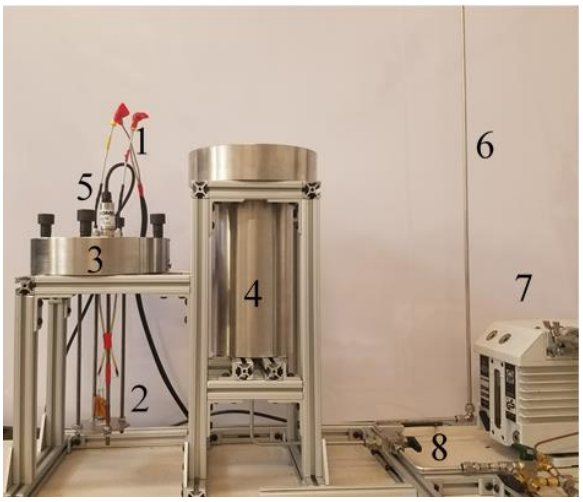

(B).

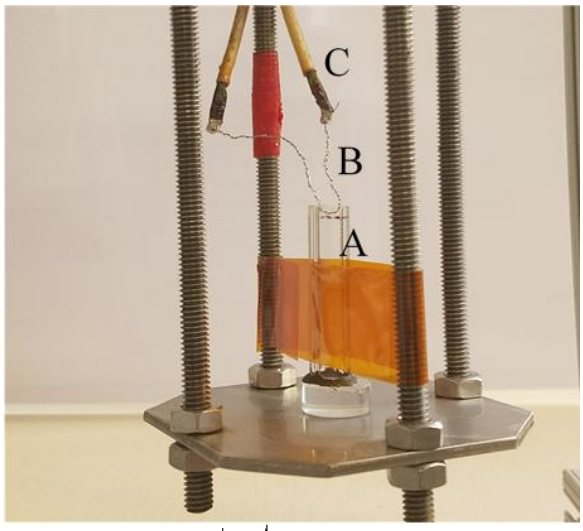

(C).

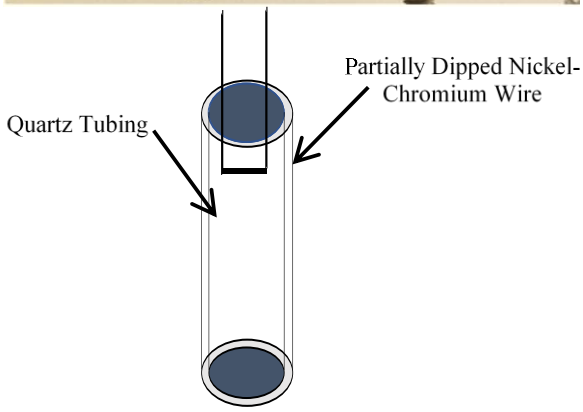

Figure 1. Experimental Setup. (A). General Setup (B). Propellant Holder Setup (C). Propellant Holder Schematic

3. RESULTS

The results from the linear burn rate experiments are presented here. Initially, a set of benchmark tests are performed with 13M HAN-water propellant at pressures of 200, 280, and 440 psig. These tests show good agreement with literature. Then, tests with the energetic ionic liquid monopropellant [Emim][EtSO4]-HAN are performed at pressures of 50, 100, 125, 150, 175 and 200 psig. All the tests performed within this study use approximately 1 ml of propellant, with the exact mass of propellant used in each test determined by measuring the weight of the sample.

3.1. CALCULATING LINEAR BURN RATE

Linear burn rate can be readily calculated for a propellant with constant cross-section. The linear burn rate is the change in length, or height, of propellant over a time period, as described in Equation (1). Previous studies have shown that the burn time can be determined from the pressure rise due to burning the propellant within a fixed volume [50, 51].

$$r_b = \frac{\triangle x}{\triangle t} \tag{1}$$

The change in length/height can be determined from the other known properties of the setup, according to Equation (2). Specifically, the known propellant mass, propellant density, and diameter of the sample holder are used. The density of the 13M HAN-water

is 1.57 g/cm3 and the density of the [Emim][$EtSO_4$]-HAN is 1.53 g/cm^3. The sample holder diameter is 5.9 mm. The mass of propellant used for each test is measured using a mass balance. Combining Equations (1) and (2) results in Equation (3), which is used to calculate the linear burn rate of propellant.

$$\triangle x = \frac{4m_p}{\pi \rho_p D_c^2} \tag{2}$$

$$r_b = \frac{4m_p}{\pi \rho_p D_c^2 \triangle t} \tag{3}$$

The measurement error is less than the variation of the data points at a given test condition. The measurement error for Δt and mp were used to calculate a maximum and minimum possible burning rate for each test. We find that errors in the propellant mass and burn time measurements compound to produce a ±2% error in the calculated burn rate. However, the three data points acquired at each test pressure condition vary by 3-15%, so we report the error bars in our data figures as the 95% confidence interval of the three data points.

3.2. BENCHMARK HAN-WATER RESULTS

Tests are performed with a 13.0M HAN-water mixture and compared with previous results by Katsumi, et. al.[31] to benchmark and validate the experimental setup and test procedure. Three tests are performed at 440 psig and 280 psig, and one test at 200 psig. A typical pressure profile during a 200 psig test of the 13M HAN-water solution is given in

Figure 2. There is a discontinuity in the pressure profile at 0.94 sec indicating the ignition and initiation of combustion of the propellant. The end of combustion is the discontinuity at 5.7 sec, where the pressure profile then turns into an exponential decreasing trend. This decrease in pressure depicts the heated combustion products cooling after all the propellant has been consumed. The difference between these two points is the burn time for the sample. The burn rate for the 80% HAN-water mixture at 440 psig (3.1MPa) is 283.5 ± 6.4 mm/s, 280 psig (2.0 MPa) is 124.7 ± 4.5 mm/s, and at 200 psig (1.5 MPa) is 8.6 mm/s using this experimental setup, and is depicted graphically in Figure with respect to the literature [31].

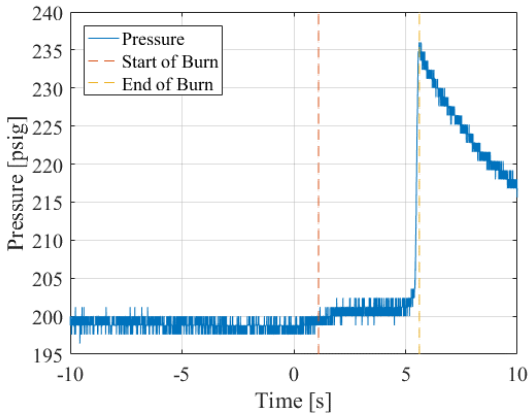

Figure 2. HAN-water pressure vs. time at 200 psig (1.5 MPa)

Results from previous experiments are plotted alongside the average burn rate measured here in Figure 3. Previous work by Katsumi et.al.[31] measured the burn rate of 80, 82.5, 85, and 90% HAN-water mixtures from 1-10 MPa. For a 80% HAN-water mixture at 200 psig (1.5 MPa), Katsumi et.al.[31] measure a burn rate of 8.4 mm/s. This result is within 0.2 mm/s (<5%) of the 8.6 mm/s burn rate measured here.

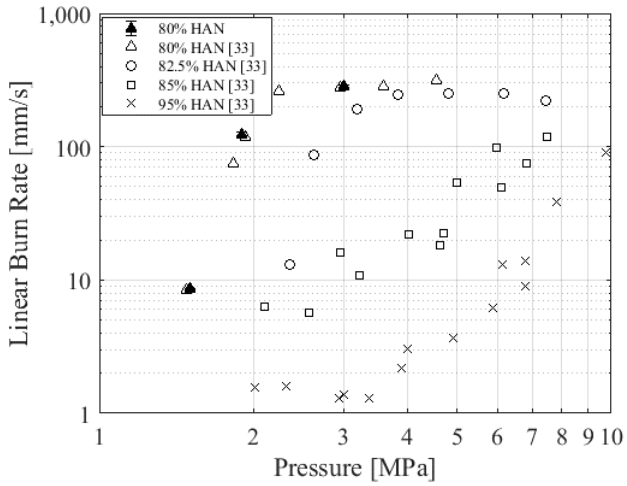

Figure 3. Comparison of linear burn rate measured with previous results for 80 – 95% aqueous HAN solutions from references [31]

3.3. [EMIM][ETSO$_4$]-HAN MONOPROPELLANT

An example pressure profile for the [Emim][EtSO4]-HAN monopropellant at 200 psig is shown in Figure 4. This figure displays the start and end of the burn time, and the pressure change throughout the test. For this propellant, there is a clear increase in pressure indicating the time when the propellant sample ignites at 0.23 sec. The [Emim][EtSO4]-HAN monopropellant causes a rise in pressure of approximately 50 psig. The pressure remains high until 1.9 sec followed by an exponential pressure decrease as the system begins to stabilize back to equilibrium. The burn time determined from similar plots for each sample, along with the measured mass and calculated burn rate are displayed in Figure 5. The average linear burn rate, determined from three tests at each starting pressure, for [Emim][EtSO$_4$]-HAN monopropellant is 26.4±2.8 mm/s, 19.7±0.9 mm/s, 10.3±0.7 mm/s, 22.4±3.5 mm/s, 18.7±2.7 mm/s and 20.0±3.9 mm/s for the starting pressures 200, 175, 150, 125, 100 and 50 psig respectively.

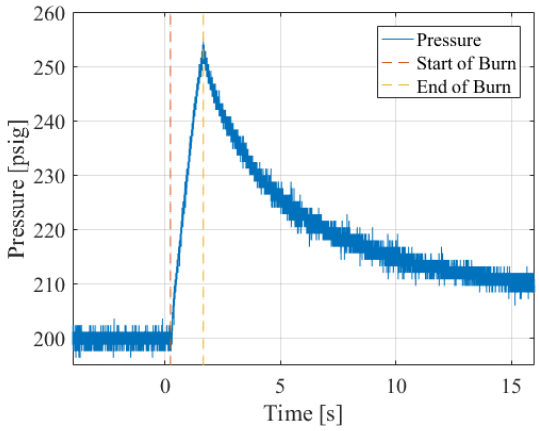

Figure 4. [Emim][$EtSO_4$]-HAN pressure vs. time at 200 psig (1.5 MPa)

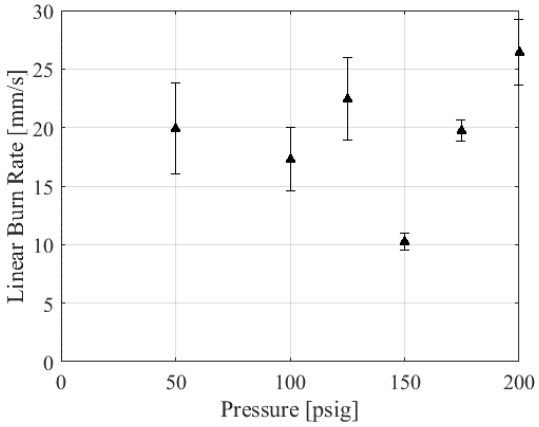

Figure 5. [Emim][$EtSO_4$]-HAN results at multiple pressures

4. DISCUSSION

Results from the preceding section are discussed, including insights for the development of a microtube thruster. The effect of pressure on the burn rate will be discussed first, followed by the effect of these results on the design of a multi-mode propulsion system.

4.1. PRESSURE TREND FOR HAN-BASED MONOPROPELLANT BURN RATE

HAN-based monopropellants have been studied previously [29, 31, 52-57]. Katsumi et.al.[31] report on a 95% by mass HAN-water mixture and show that burn rate increases with pressure for pressures above 4 MPa. A similar trend is reported for 85% HAN-water for pressure above 3.5 MPa. But at lower pressures the burn rate is approximately constant at 1.5 and 6.0 mm/s for 95% and 85% HAN-water, respectively. Amrousse et al.[52] report on monopropellant mixtures of HAN, ammonium nitrate (AN), water, and methanol named SHP163 (95/5/8/21 by moles per reaction) and a control propellant (95/5/8/0). Results show SHP163 burn rate increases from 0.3 to 50 mm/s as pressure increases from 2 to 6 MPa. The burning rate of the control propellant increases from 7 to 300 mm/s over the same range, but for pressure below 2 MPa the burn rate is constant at 7 mm/s. Katsumi et al. [53] also report on SHP163 and the same control propellant along with another named SHP069 (95/5/8/8 by moles per reaction). Results show SHP069 burn rate increases from 3 to 200 mm/s for pressures 1.5 to 7 MPa, and for pressures less than 5 MPa the burning rate is constant at 5 mm/s. Vosen [54] reports on turbulent combustion of a mixture of HAN and triethanolammonium nitrate (TEAN) named LP1846, and 62.6% aqueous HAN solution, and shows that burn rate decreases for both propellants from about 250 mm/s to 80 mm/s as pressure increases from 6 MPa to 30 MPa. Vosen [55] also reports on the laminar burning velocity of the HAN-based liquid propellant LP1846 within the pressure range of 6.7 to 34 MPa, with results showing a laminar burning rate between 26.7 and 27.9 mm/s at pressures of 30 to 34 MPa. Vosen [56] reported on the concentration and pressure effects on aqueous HAN solution decomposition rates for mixtures of 3.12 to 13.0 molar aqueous HAN solutions over

pressures of 6 to 34 MPa. This report concluded that the overall decomposition rate was a function of the pressure and the concentration of the monopropellant mixtures. Kondrikov et al. [57] reports results for crystalline HAN, monopropellant mixture of 57.5% HAN, 5% water, and 37.5% monoethanolamine nitrate (EAN), and 9.2 molar and 8.6 molar aqueous HAN solutions within the pressure range of 0.1 to 36 MPa. Results showed an increase in linear burning rate from greater than 200 to 600 mm/s in the pressure regime of 2 to 12 MPa for the monopropellant mixture of HAN, EAN, and water, and an increase in burning rate from 0.1 to 50 mm/s for the pressure range of 0.5 to 11 MPa. Mundahl et. al. [29] report on a mixture of 41% [Emim][EtSO4] and 59% HAN by mass for two different heating element geometries within the pressure range of 0.5 to 1.5 MPa. A relatively constant linear burn rate is observed with an average burning rate of 41.4 mm/s for the most submerged heating element geometry.

In many HAN-based monopropellants it is observed that below a particular pressure (in most cases 2-4 MPa) the burn rate remains relatively constant, and this trend also appears to be present in the data of Figure 5. Constant burn rate at low pressure was observed in HAN-water mixtures by Katsumi et.al. [31], HAN-AN-water mixtures by Amrousse et al. [52], and Katsumi et al. for SHP069, SHP163, and a control monopropellant mixture [53]. The data presented in Figure 5 is for pressure below 1.5 MPa, and exhibits an almost constant trend with pressure. Across all pressures tested the average linear burn rate is 19.6 mm/s with an average deviation of about 17%. The largest difference from the average burn rate is 50% at 150 psig (1.1 MPa). Still this difference is significantly less than what is observed in the literature for HAN-based monopropellants at higher pressure, where linear burn rate often increases by an order of magnitude or more.

The multi-mode propellant appears to conform with many previous HAN-based monopropellants by exhibiting a nearly constant linear burn rate at low pressure with a magnitude (~20 mm/s) similar to other HAN-based monopropellants in the same pressure range (~5-50 mm/s).

The results of Figure 5 also compare well with previous tests of the multi-mode propellant. Previous tests used a similar linear burn rate experiment, but fully dipped the nichrome wire into the propellant sample [29]. Results from those previous tests predicted linear burn rates 75% higher than those of Figure 5. This may be expected since a fully-dipped nichrome wire would ignite the propellant everywhere in the propellant holder (as opposed to just at the surface). This would give rise to an artificially high linear burn rate as all the propellant burns at once instead of a linear progression. The burn rate measured in those tests was also nearly constant across the same pressure range tested in this analysis, 50 to 200 psig, with an average burning rate of 41.4 mm/s. It is interesting to note that those previous results indicate a minimum burn rate at 150 psig, similar to the results in Figure 5.

There is a non-negligible pressure rise during the linear burn rate experiment, but maximum pressure is still well below the regime where strong pressure dependence on burn rate is expected (<2 MPa). As shown in Figure 2 and Figure 4, when the propellant ignites and generates gaseous products the pressure in the vessel increases by up to 25%. We report the initial pressure as the test condition, but clearly the pressure increases during the test. However, even with this pressure increase the benchmark data agree well (within 5%) with literature (Figure 3). And as discussed in the preceding paragraph, the multi-

mode propellant exhibits nearly constant burn rate with pressure within the pressure range being tested, a result that is similar to many other HAN-based monopropellants.

4.2. IMPACT OF BURN RATE RESULTS ON CATALYTIC MICROTUBE MICROTHRUSTER DESIGN

The linear burn rate is a useful parameter in the design of chemical monopropellant thrusters. The most obvious application to thruster design is in the prevention of flashback into the feed system or propellant tank. Since the goal of the sample holder in the linear burn rate experiments is to minimize the effect of heat transfer in the quenching of the propellant decomposition reaction, the linear burn rate results can be used to obtain an estimate of the required minimum feed rate in a tube or other geometry. A recent multi-mode concept is to integrate together a catalytic microtube with an electrospray thruster [49]. So here we use the linear burn rate obtained from experiment to define a minimum flow rate as a function of tube diameter to feed the propellant to the catalytic microtube thruster at a rate greater than the burn rate of the propellant. The minimum flow rate is calculated for tube inner diameters of 0.1 to 10 mm using Equation (4) and is shown in Figure 6.

$$\dot{m}_p = \frac{\pi}{4} \rho_p r_b D_t^2 \tag{4}$$

The two lines shown in Figure 6 correspond to the largest range of possible minimum burn rates determined for the [Emim][EtSO4]-HAN propellant in the tested pressure range of 50 to 200 psig. Using these results at 200 psig, the minimum flow rate

required is between 0.12 and 0.35 mg/s for a tube of 0.1 mm inner diameter and 1.16 to 3.51 g/s for a tube of 10 mm inner diameter. For a microtube type thruster, which does not include a nozzle, the specific impulse of this propellant is predicted to be 170 seconds [11]. This corresponds to a minimum thrust level between 0.19 and 0.59 mN for a 0.1 mm inner diameter tube and between 1.93 and 5.85 N for a 10 mm diameter tube. Or, stated in a way more representative of design selection, if a thruster of 1.93 to 5.85 N thrust per emitter is desired, the feed tube can be a maximum of 10 mm inner diameter. If the diameter is larger, then the mass flow rate would be too low and the propellant would burn back into the propulsion system.

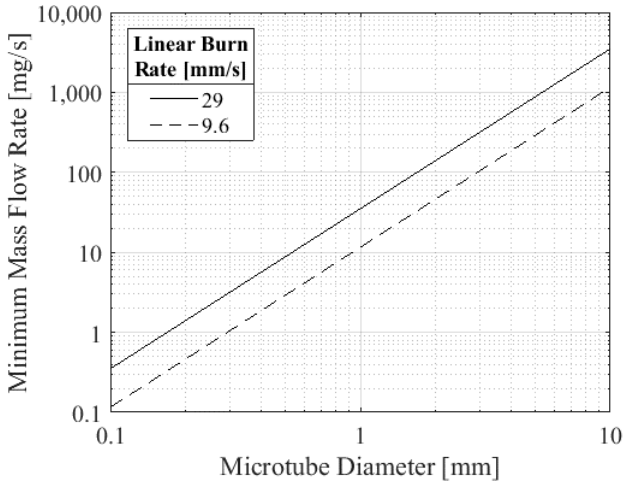

Figure 6. Minimum required propellant mass flow rate to prevent flashback into feed system for [Emim][$EtSO_4$]-HAN propellant

5. CONCLUSION

From the results provided and the following discussion, it was determined that the linear burn rate of aqueous HAN solutions tested in this linear burning rate experiment are

similar to the discussed literature, to within 5%. Also, it was observed that the [Emim][EtSO4]-HAN monopropellant mixture is readily ignited in the pressure regime tested in this linear burn rate experiment, with a rapid pressure rise. This monopropellant mixture has linear burn rate in the pressure range tested, 50 to 200 psig, between 9.6 and 29 mm/s with 95% confidence. From this result, it was concluded that the minimum flow rate required for a 0.1 mm microtube is between 0.12 to 0.35 mg/s, and 1.16 to 3.51 g/s for a tube of 10 mm inner diameter. These discoveries should help improve the results of the multi-mode propulsion system under design, and improve the system final performance.

ACKNOWLEDGMENTS

The authors would like to thank the researchers of the Aerospace Plasma Laboratory for their assistance throughout this experiment, and providing insightful information. The authors thank the technicians within the department machine shop for their assistance in the manufacturing process of this experiment. Support for this work was provided through the NASA Marshall Space Flight Center, NASA grant NNM15AA09A, and the Air Force University Nanosatellite Program through the Utah State University Research Foundation, grant CP0039814. Additional support was provided by NASA Goddard Space Flight Center through the NASA Undergraduate Student Instrument Project grant NNX16AI85A, and the University of Missouri System Fast Track Program.

REFERENCES

[1] T. Rexius and M. Holmes, "Mission Capability Gains from Multi-Mode Propulsion Thrust Profile Variations for a Plane Change Maneuver," *AIAA Modeling and Simulation Technologies Conference*, American Institute of Aeronautics and Astronautics, 2011.
doi:10.2514/6.2011-6431

[2] J. Hass and M. Holmes, *Multi-Mode Propulsion System for the Expansion of Small Satellite Capabilities*, 2010.

[3] B. R. Donius and J. L. Rovey, "Ionic Liquid Dual-Mode Spacecraft Propulsion Assessment," *Journal of Spacecraft and Rockets*, Vol. 48, No. 1, pp. 110-123, 2011.
doi: 10.2514/1.49959

[5] S. P. Berg and J. L. Rovey, "Assessment of Multimode Spacecraft Micropropulsion Systems," *Journal of Spacecraft and Rockets*, Vol. 54, No. 3, pp. 592-601, 2017.
doi: 10.2514/1.A33649

[6] S. P. Berg and J. L. Rovey, "Assessment of High-Power Electric Multi-Mode Spacecraft Propulsion Concepts," *33rd Internation Electric Propulsion Conference*, 2013.

[8] C. A. Kluever, "Optimal Geostationary Orbit Transfers Using Onboard Chemical-Electric Propulsion," *Journal of Spacecraft and Rockets*, Vol. 49, No. 6, pp. 1174-1182, 2012.
doi: 10.2514/1.A32213

[9] D. Y. Oh, T. Randolph, S. Kimbrel and M. Martinez-Sanchez, "End-to-End Optimization of Chemical-Electric Orbit-Raising Missions," *Journal of Spacecraft and Rockets*, Vol. 41, No. 5, pp. 831-839, 2004.
doi: 10.2514/1.13096

[10] S. R. Oleson, R. M. Myers, C. A. Kluever, J. P. Riehl and F. M. Curran, "Advanced Propulsion for Geostationary Orbit Insertion and North-South Station Keeping," *Journal of Spacecraft and Rockets*, Vol. 34, No. 1, pp. 22-28, 1997.
doi: 10.2514/2.3187

[11] S. P. Berg and J. L. Rovey, "Assessment of Imidazole-Based Ionic Liquids as Dual-Mode Spacecraft Propellants," *Journal of Propulsion and Power*, Vol. 29, No. 2, pp. 339-351, 2013.
doi: 10.2514/1.B34341

[12] Y.-h. Chiu and R. A. Dressler, *Ionic Liquids for Space Propulsion*, ACS Publications, Washington, D. C., 2007.

[13] M. Gamero-Castaño, "Characterization of a Six-Emitter Colloid Thruster Using a Torsional Balance," *Journal of Propulsion and Power*, Vol. 20, No. 4, pp. 736-741, 2004.
10.2514/1.2470

[14] G. A. Boyarko, C.-J. Sung and S. J. Schneider, "Catalyzed Combustion of Hydrogen–Oxygen in Platinum Tubes for Micro-Propulsion Applications," *Proceedings of the Combustion Institute*, Vol. 30, No. 2, pp. 2481-2488, 2005.
https://doi.org/10.1016/j.proci.2004.08.203

[15] C. A. Mento, C.-J. Sung, A. F. Ibarreta and S. J. Schneider, "Catalyzed Ignition of Using Methane/Hydrogen Fuel in a Microtube for Microthruster Applications," *Journal of Propulsion and Power*, Vol. 25, No. 6, pp. 1203-1210, 2009.
doi: 10.2514/6.2006-4871

[16] S. J. Volchko, C.-J. Sung, Y. Huang and S. J. Schneider, "Catalytic Combustion of Rich Methane/Oxygen Mixtures for Micropropulsion Applications," *Journal of Propulsion and Power*, Vol. 22, No. 3, pp. 684-693, 2006.
doi: 10.2514/1.19809

[17] M. S. Alexander, J. Stark, K. L. Smith, B. Stevens and B. Kent, "Electrospray Performance of Microfabricated Colloid Thruster Arrays," *Journal of Propulsion and Power*, Vol. 22, No. 3, pp. 620-627, 2006.
doi: 10.2514/1.15190

[19] P. S. George and B. Oscar, *Rocket Propulsion Elements*, Wiley, OSCAR BIBLARZ, 2001.

[20] D. Amariei, L. Courthéoux, S. Rossignol, Y. Batonneau, C. Kappenstein, M. Ford and N. Pillet, "Influence of Fuel on Thermal and Catalytic Decompositions of Ionic Liquid Monopropellants," *41st AIAA/ASME/SAE/ASEE Joint Propulsion Conference & Exhibit*, American Institute of Aeronautics and Astronautics, 2005.
doi:10.2514/6.2005-3980

[21] K. Anflo and T.-A. Grönland, "Towards Green Propulsion for Spacecraft with Adn-Based Monopropellants," *38th AIAA/ASME/SAE/ASEE Joint Propulsion Conference & Exhibit*, American Institute of Aeronautics and Astronautics, 2002.
doi:10.2514/6.2002-3847

[22] K. Anflo, S. Persson, P. Thormahlen, G. Bergman and T. Hasanof, "Flight Demonstration of an Adn-Based Propulsion System on the Prisma Satellite," *42nd AIAA/ASME/SAE/ASEE Joint Propulsion Conference & Exhibit*, American Institute of Aeronautics and Astronautics, 2006.
doi:10.2514/6.2006-5212

[23] B. Slettenhaar, J. Zevenbergen, H. Pasman, A. Maree and J. Moerel, "Study on Catalytic Ignition of Hnf Based Non Toxic Monopropellants," *39th AIAA/ASME/SAE/ASEE Joint Propulsion Conference and Exhibit*, AIAA Paper 2003-4920, 2003.
doi: 10.2514/6.2003-4920

[24] C. H. McLean, "Green Propellant Infusion Mission Program Development and Technology Maturation," *50th AIAA/ASME/SAE/ASEE Joint Propulsion Conference*, American Institute of Aeronautics and Astronautics, 2014.
doi:10.2514/6.2014-3481

[25] K. Anflo and R. Möllerberg, "Flight Demonstration of New Thruster and Green Propellant Technology on the Prisma Satellite," *Acta Astronautica*, Vol. 65, No. 9, pp. 1238-1249, 2009. https://doi.org/10.1016/j.actaastro.2009.03.056

[26] S. P. Berg and J. L. Rovey, "Decomposition of Monopropellant Blends of Hydroxylammonium Nitrate and Imidazole-Based Ionic Liquid Fuels," *Journal of Propulsion and Power*, Vol. 29, No. 1, pp. 125-135, 2012.
doi: 10.2514/1.B34584

[27] S. P. Berg, J. Rovey, B. Prince, S. Miller and R. Bemish, "Electrospray of an Energetic Ionic Liquid Monopropellant for Multi-Mode Micropropulsion Applications," *51st AIAA/SAE/ASEE Joint Propulsion Conference*, American Institute of Aeronautics and Astronautics, 2015.
doi:10.2514/6.2015-4011

[29] A. Mundahl, S. P. Berg and J. Rovey, "Linear Burn Rates of Monopropellants for Multi-Mode Micropropulsion," *52nd AIAA/SAE/ASEE Joint Propulsion Conference*, American Institute of Aeronautics and Astronautics, 2016.
doi:10.2514/6.2016-4579

[30] Y.-P. Chang, "Combustion Behavior of Han-Based Liquid Propellants," Mechanical Engineering, The Pennsylvania State University, 2002.

[31] T. Katsumi, K. Hori, R. Matsuda and T. Inoue, "Combustion Wave Structure of Hydroxylammonium Nitrate Aqueous Solutions," *46th AIAA/ASME/SAE/ASEE Joint Propulsion Conference & Exhibit*, American Institute of Aeronautics and Astronautics, 2010.
doi:10.2514/6.2010-6900

[32] K. W. McCown, G. Homan-Cruz and E. L. Petersen, "Effects of Nano-Scale Additives and Methanol on the Linear Burning Rates of Aqueous Han Solutions," *50th AIAA/ASME/SAE/ASEE Joint Propulsion Conference*, American Institute of Aeronautics and Astronautics, 2014.
doi:10.2514/6.2014-3566

[34] S. P. Berg and J. Rovey, "Decomposition of a Double Salt Ionic Liquid Monopropellant on Heated Metallic Surfaces," *52nd AIAA/SAE/ASEE Joint Propulsion Conference*, American Institute of Aeronautics and Astronautics, 2016. doi:10.2514/6.2016-4578

[45] C. A. Kluever, "Spacecraft Optimization with Combined Chemical-Electric Propulsion," *Journal of Spacecraft and Rockets*, Vol. 32, No. 2, pp. 378-380, 1995. doi: 10.2514/3.26623

[46] L. M. Mailhe and S. D. Heister, "Design of a Hybrid Chemical/Electric Propulsion Orbital Transfer Vehicle," *Journal of Spacecraft and Rockets*, Vol. 39, No. 1, pp. 131-139, 2002. doi: 10.2514/2.3791

[47] A. J. Mundahl, S. P. Berg, J. Rovey, M. Huang, K. Woelk, D. Wagle and G. Baker, "Characterization of a Novel Ionic Liquid Monopropellant for Multi-Mode Propulsion," *53rd AIAA/SAE/ASEE Joint Propulsion Conference*, American Institute of Aeronautics and Astronautics, 2017. doi:10.2514/6.2017-4756

[48] S. P. Berg, "Development of Ionic Liquid Multi-Mode Spacecraft Micropropulsion Systems," Dissertation, Mechanical and Aerospace Department, Missouri University of Science and Technology, 2015.

[49] S. P. Berg and J. L. Rovey, "Design and Development of a Multi-Mode Monopropellant Electrospray Mircropropulsion System," *30th AIAA/USU Conference on Small Satellites*, to be presented, 2016.

[50] W. C. Warren, "Experimental Techniques for the Study of Liquid Monopropellant Combustion," Mechanical Engineering, Texas A&M University, 2012.

[51] W. C. Warren, McCown, K., and Peterson, E. L., "Experimental Techniques for the Study of Ionic Liquid Combustion at High Pressure," *Spring Technical Meeting the Central States Section of the Combustion Institute*, 2012.

[52] R. Amrousse, T. Katsumi, N. Azuma and K. Hori, "Hydroxylammonium Nitrate (Han)-Based Green Propellant as Alternative Energy Resource for Potential Hydrazine Substitution: From Lab Scale to Pilot Plant Scale-Up," *Combustion and Flame*, Vol. 176, No. Supplement C, pp. 334-348, 2017. https://doi.org/10.1016/j.combustflame.2016.11.011

[53] T. Katsumi, T. Inoue, J. Nakatsuka, K. Hasegawa, K. Kobayashi, S. Sawai and K. Hori, "Han-Based Green Propellant, Application, and Its Combustion Mechanism," *Combustion, Explosion, and Shock Waves*, Vol. 48, No. 5, pp. 536-543, 2012. 10.1134/S001050821205005X

[54] S. R. Vosen, "The Burning Rate of Hydroxylammonium Nitrate-Based Liquid Propellants," *Symposium (International) on Combustion*, Vol. 22, No. 1, pp. 1817-1825, 1989.
https://doi.org/10.1016/S0082-0784(89)80195-X

[55] S. R. Vosen, "Hydroxylammonium Nitrate-Based Liquid Propellant Combustion-Interpretation of Strand Burner Data and the Laminar Burning Velocity," *Combustion and Flame*, Vol. 82, No. 3, pp. 376-388, 1990.
https://doi.org/10.1016/0010-2180(90)90009-G

[56] S. R. Vosen, "Concentration and Pressure Effects on the Decomposition Rate of Aqueous Hydroxylammonium Nitrate Solutions," *Combustion Science and Technology*, Vol. 68, No. 4-6, pp. 85-99, 1989.
10.1080/00102208908924070

[57] B. N. Kondrikov, V. É. Annikov, V. Y. Egorshev and L. T. De Luca, "Burning of Hydroxylammonium Nitrate," *Combustion, Explosion and Shock Waves*, Vol. 36, No. 1, pp. 135-145, 2000.
10.1007/BF02701522

SECTION

2. CONCLUSION

2.1. CONCLUSIONS FROM PROP CHARACTERIZATION PAPER

Five propellants were experimentally characterized in this work with envisioned application as multi-mode micropropulsion propellants, four of which (B, C, D, E) were new propellants with a novel ionic liquid fuel, [Cho][NO_3] – glycerol. The fifth propellant (A) is our previously investigated and promising propellant that is a mixture of [Emim][$EtSO_4$]-HAN. Propellants D and E used AN oxidizer with the new fuel, but required high temperatures to initiate decomposition and are unlikely to be viable for the application. Propellants B and C used HAN oxidizer with the new fuel. Propellants B and C have significantly lower self-heating rates, approximately 240 $^oC/s$ lower, than the self-heating rate of propellant A at similar heat flux values. The heating rates for propellant B on rhenium and titanium foils were both determined to be approximately 40 $^oC/s$, and the decomposition temperatures were approximately 158 ^oC and 173 ^oC respectively. These decomposition temperatures are both in close proximity to the decomposition of HAN at 165 ^oC, but are higher than the decomposition temperatures obtained for propellant A in this and previous studies. When heated on rhenium and titanium foils, propellant C experienced endothermic decomposition events, and an unquantifiable exothermic decomposition event on platinum foil. Therefore, further study of this propellant mixture with higher heat fluxes into the propellant sample are required to obtain quantifiable exothermic decomposition events.

Theoretically the novel ionic liquid binary mixtures, propellants B and C, are capable of performing better than propellant A with respect to I_{sp}, approximately 280 versus 250 seconds, while operating at lower or similar combustion temperatures, 1300K versus 1900K. Therefore, design studies taking power requirements, total mass, available momentum change, and performance characteristics are required to determine which monopropellant mixture is ideal for a multi-mode micropropulsion system. However, with this initial study, the results indicate [Emim][$EtSO_4$]-HAN with platinum catalyst is still the most promising as a multi-mode micropropulsion propellant and catalyst material combination.

2.2. CONCLUSIONS FROM LINEAR BURN RATE PAPER.

From the results provided and the following discussion, it was determined that the linear burn rate of aqueous HAN solutions tested in this linear burning rate experiment are similar to the discussed literature. Also, it was observed that the specified [Emim][EtSO4]-HAN monopropellant mixture is readily ignited in the pressure regime utilized in this linear burn rate experiment with a rapid pressure rise. Also, this monopropellant mixture's linear burn rate utilizing dipped nickel-chromium wire at 200 psig is between 24 and 29 mm/s with 95% confidence. From this result, it was concluded that the minimum flow rate required for a 0.1 mm microtube is 0.31 mg/s, and 3180 mg/s for a tube of 10 mm inner diameter. These discoveries should help improve the results of the multi-mode prop system under design, and improve the system final performance.

BIBLIOGRAPHY

[1] T. Rexius and M. Holmes, "Mission Capability Gains from Multi-Mode Propulsion Thrust Profile Variations for a Plane Change Maneuver," *AIAA Modeling and Simulation Technologies Conference*, American Institute of Aeronautics and Astronautics, 2011.
doi:10.2514/6.2011-6431

[2] J. Hass and M. Holmes, *Multi-Mode Propulsion System for the Expansion of Small Satellite Capabilities*, 2010.

[3] B. R. Donius and J. L. Rovey, "Ionic Liquid Dual-Mode Spacecraft Propulsion Assessment," *Journal of Spacecraft and Rockets*, Vol. 48, No. 1, pp. 110-123, 2011.
doi: 10.2514/1.49959

[4] B. Donius and J. Rovey, "Analysis and Prediction of Dual-Mode Chemical and Electric Ionic Liquid Propulsion Performance," *48th AIAA Aerospace Sciences Meeting Including the New Horizons Forum and Aerospace Exposition*, American Institute of Aeronautics and Astronautics, 2010.
doi:10.2514/6.2010-1328

[5] S. P. Berg and J. L. Rovey, "Assessment of Multimode Spacecraft Micropropulsion Systems," *Journal of Spacecraft and Rockets*, Vol. 54, No. 3, pp. 592-601, 2017.
doi: 10.2514/1.A33649

[6] S. P. Berg and J. L. Rovey, "Assessment of High-Power Electric Multi-Mode Spacecraft Propulsion Concepts," *33rd Internation Electric Propulsion Conference*, 2013.

[7] C. A. Kluever, "Spacecraft Optimization with Combined Chemical-Electric Propulsion," *Journal of Spacecraft and Rockets*, Vol. 32, No. 2, pp. 378-379, 1995.
doi: 10.2514/3.26623

[8] C. A. Kluever, "Optimal Geostationary Orbit Transfers Using Onboard Chemical-Electric Propulsion," *Journal of Spacecraft and Rockets*, Vol. 49, No. 6, pp. 1174-1182, 2012.
doi: 10.2514/1.A32213

[9] D. Y. Oh, T. Randolph, S. Kimbrel and M. Martinez-Sanchez, "End-to-End Optimization of Chemical-Electric Orbit-Raising Missions," *Journal of Spacecraft and Rockets*, Vol. 41, No. 5, pp. 831-839, 2004.
doi: 10.2514/1.13096

[10] S. R. Oleson, R. M. Myers, C. A. Kluever, J. P. Riehl and F. M. Curran, "Advanced Propulsion for Geostationary Orbit Insertion and North-South Station Keeping," *Journal of Spacecraft and Rockets,* Vol. 34, No. 1, pp. 22-28, 1997.
doi: 10.2514/2.3187

[11] S. P. Berg and J. L. Rovey, "Assessment of Imidazole-Based Ionic Liquids as Dual-Mode Spacecraft Propellants," *Journal of Propulsion and Power,* Vol. 29, No. 2, pp. 339-351, 2013.
doi: 10.2514/1.B34341

[12] Y.-h. Chiu and R. A. Dressler, *Ionic Liquids for Space Propulsion,* ACS Publications, Washington, D. C., 2007.

[13] M. Gamero-Castaño, "Characterization of a Six-Emitter Colloid Thruster Using a Torsional Balance," *Journal of Propulsion and Power,* Vol. 20, No. 4, pp. 736-741, 2004.
10.2514/1.2470

[14] G. A. Boyarko, C.-J. Sung and S. J. Schneider, "Catalyzed Combustion of Hydrogen–Oxygen in Platinum Tubes for Micro-Propulsion Applications," *Proceedings of the Combustion Institute,* Vol. 30, No. 2, pp. 2481-2488, 2005.
https://doi.org/10.1016/j.proci.2004.08.203

[15] C. A. Mento, C.-J. Sung, A. F. Ibarreta and S. J. Schneider, "Catalyzed Ignition of Using Methane/Hydrogen Fuel in a Microtube for Microthruster Applications," *Journal of Propulsion and Power,* Vol. 25, No. 6, pp. 1203-1210, 2009.
doi: 10.2514/6.2006-4871

[16] S. J. Volchko, C.-J. Sung, Y. Huang and S. J. Schneider, "Catalytic Combustion of Rich Methane/Oxygen Mixtures for Micropropulsion Applications," *Journal of Propulsion and Power,* Vol. 22, No. 3, pp. 684-693, 2006.
doi: 10.2514/1.19809

[17] M. S. Alexander, J. Stark, K. L. Smith, B. Stevens and B. Kent, "Electrospray Performance of Microfabricated Colloid Thruster Arrays," *Journal of Propulsion and Power,* Vol. 22, No. 3, pp. 620-627, 2006.
doi: 10.2514/1.15190

[18] S. P. Berg and J. L. Rovey, "Design and Development of a Multi-Mode Monopropellant Electrospray Mircropropulsion System," 2016.

[19] P. S. George and B. Oscar, *Rocket Propulsion Elements,* Wiley, OSCAR BIBLARZ, 2001.

[20] D. Amariei, L. Courthéoux, S. Rossignol, Y. Batonneau, C. Kappenstein, M. Ford and N. Pillet, "Influence of Fuel on Thermal and Catalytic Decompositions of Ionic Liquid Monopropellants," *41st AIAA/ASME/SAE/ASEE Joint Propulsion Conference & Exhibit*, American Institute of Aeronautics and Astronautics, 2005. doi:10.2514/6.2005-3980

[21] K. Anflo and T.-A. Grönland, "Towards Green Propulsion for Spacecraft with Adn-Based Monopropellants," *38th AIAA/ASME/SAE/ASEE Joint Propulsion Conference & Exhibit*, American Institute of Aeronautics and Astronautics, 2002. doi:10.2514/6.2002-3847

[22] K. Anflo, S. Persson, P. Thormahlen, G. Bergman and T. Hasanof, "Flight Demonstration of an Adn-Based Propulsion System on the Prisma Satellite," *42nd AIAA/ASME/SAE/ASEE Joint Propulsion Conference & Exhibit*, American Institute of Aeronautics and Astronautics, 2006. doi:10.2514/6.2006-5212

[23] B. Slettenhaar, J. Zevenbergen, H. Pasman, A. Maree and J. Moerel, "Study on Catalytic Ignition of Hnf Based Non Toxic Monopropellants," *39th AIAA/ASME/SAE/ASEE Joint Propulsion Conference and Exhibit*, AIAA Paper 2003-4920, 2003. doi: 10.2514/6.2003-4920

[24] C. H. McLean, "Green Propellant Infusion Mission Program Development and Technology Maturation," *50th AIAA/ASME/SAE/ASEE Joint Propulsion Conference*, American Institute of Aeronautics and Astronautics, 2014. doi:10.2514/6.2014-3481

[25] K. Anflo and R. Möllerberg, "Flight Demonstration of New Thruster and Green Propellant Technology on the Prisma Satellite," *Acta Astronautica*, Vol. 65, No. 9, pp. 1238-1249, 2009. https://doi.org/10.1016/j.actaastro.2009.03.056

[26] S. P. Berg and J. L. Rovey, "Decomposition of Monopropellant Blends of Hydroxylammonium Nitrate and Imidazole-Based Ionic Liquid Fuels," *Journal of Propulsion and Power*, Vol. 29, No. 1, pp. 125-135, 2012. doi: 10.2514/1.B34584

[27] S. P. Berg, J. Rovey, B. Prince, S. Miller and R. Bemish, "Electrospray of an Energetic Ionic Liquid Monopropellant for Multi-Mode Micropropulsion Applications," *51st AIAA/SAE/ASEE Joint Propulsion Conference*, American Institute of Aeronautics and Astronautics, 2015. doi:10.2514/6.2015-4011

[28] S. P. Berg and J. Rovey, "Decomposition of a Double Salt Ionic Liquid Monopropellant in a Microtube for Multi-Mode Micropropulsion Applications," *53rd AIAA/SAE/ASEE Joint Propulsion Conference*, American Institute of Aeronautics and Astronautics, 2017.
doi:10.2514/6.2017-4755

[29] A. Mundahl, S. P. Berg and J. Rovey, "Linear Burn Rates of Monopropellants for Multi-Mode Micropropulsion," *52nd AIAA/SAE/ASEE Joint Propulsion Conference*, American Institute of Aeronautics and Astronautics, 2016.
doi:10.2514/6.2016-4579

[30] Y.-P. Chang, "Combustion Behavior of Han-Based Liquid Propellants," Mechanical Engineering, The Pennsylvania State University, 2002.

[31] T. Katsumi, K. Hori, R. Matsuda and T. Inoue, "Combustion Wave Structure of Hydroxylammonium Nitrate Aqueous Solutions," *46th AIAA/ASME/SAE/ASEE Joint Propulsion Conference & Exhibit*, American Institute of Aeronautics and Astronautics, 2010.
doi:10.2514/6.2010-6900

[32] K. W. McCown, G. Homan-Cruz and E. L. Petersen, "Effects of Nano-Scale Additives and Methanol on the Linear Burning Rates of Aqueous Han Solutions," *50th AIAA/ASME/SAE/ASEE Joint Propulsion Conference*, American Institute of Aeronautics and Astronautics, 2014.
doi:10.2514/6.2014-3566

[33] J. Hass and M. Holmes, *Multi-Mode Propulsion System for the Expansion of Small Satellite Capabilities*, NATO, 2010.

[34] S. P. Berg and J. Rovey, "Decomposition of a Double Salt Ionic Liquid Monopropellant on Heated Metallic Surfaces," *52nd AIAA/SAE/ASEE Joint Propulsion Conference*, American Institute of Aeronautics and Astronautics, 2016.
doi:10.2514/6.2016-4578

[35] Z.-H. Zhang, Z.-C. Tan, L.-X. Sun, Y. Jia-Zhen, X.-C. Lv and Q. Shi, "Thermodynamic Investigation of Room Temperature Ionic Liquid: The Heat Capacity and Standard Enthalpy of Formation of Emies," *Thermochimica Acta*, Vol. 447, No. 2, pp. 141-146, 2006.

[36] P. S. o. A. a. Astronautics, *Propulsion Web Page*, Purdue School of Aeronautics and Astronautics,

[37] S. Berg and J. Rovey, *Dual-Mode Propellant Properties and Performance Analysis of Energetic Ionic Liquids*, 2012.

[38] N. Klein, "Liquid Propellant for Usin in Guns - a Review," Rept. BRL-TR-2641, 1985.

[39] C. P. I. A. C. MD., *Cpia/M5 Liquid Propellant Engine Manual October 1992 Supplement (Unit No. 228)*, Defense Technical Information Center, 1992.

[40] K. Anflo, S. Persson, P. Thormahlen, G. Bergman and T. Hasanof, *Flight Demonstration of an Adn-Based Propulsion System on the Prisma Satellite*, 2006.

[41] B. G. Pfrommer, F. Mauri and S. G. Louie, "Nmr Chemical Shifts of Ice and Liquid Water: The Effects of Condensation," *Journal of the American Chemical Society*, Vol. 122, No. 1, pp. 123-129, 2000.

[42] R. Eloirdi, S. Rossignol, C. Kappenstein, D. Duprez and N. Pillet, "Design and Use of a Batch Reactor for Catalytic Decomposition of Propellants," *Journal of Propulsion and Power*, Vol. 19, No. 2, pp. 213-219, 2003.

[43] E. W. Schmidt, *Hydroxylammonium Nitrate Compatibility Tests with Various Materials-a Liquid Propellant Study*, DTIC Document, 1990.

[44] C. H. McLean, *Green Propellant Infusion Mission Program Development and Technology Maturation*, 2014.

[45] C. A. Kluever, "Spacecraft Optimization with Combined Chemical-Electric Propulsion," *Journal of Spacecraft and Rockets*, Vol. 32, No. 2, pp. 378-380, 1995. doi: 10.2514/3.26623

[46] L. M. Mailhe and S. D. Heister, "Design of a Hybrid Chemical/Electric Propulsion Orbital Transfer Vehicle," *Journal of Spacecraft and Rockets*, Vol. 39, No. 1, pp. 131-139, 2002.
doi: 10.2514/2.3791

[47] A. J. Mundahl, S. P. Berg, J. Rovey, M. Huang, K. Woelk, D. Wagle and G. Baker, "Characterization of a Novel Ionic Liquid Monopropellant for Multi-Mode Propulsion," *53rd AIAA/SAE/ASEE Joint Propulsion Conference*, American Institute of Aeronautics and Astronautics, 2017.
doi:10.2514/6.2017-4756

[48] S. P. Berg, "Development of Ionic Liquid Multi-Mode Spacecraft Micropropulsion Systems," Dissertation, Mechanical and Aerospace Department, Missouri University of Science and Technology, 2015.

[49] S. P. Berg and J. L. Rovey, "Design and Development of a Multi-Mode Monopropellant Electrospray Mircropropulsion System," *30th AIAA/USU Conference on Small Satellites*, to be presented, 2016.

[50] W. C. Warren, "Experimental Techniques for the Study of Liquid Monopropellant Combustion," Mechanical Engineering, Texas A&M University, 2012.

[51] W. C. Warren, McCown, K., and Peterson, E. L., "Experimental Techniques for the Study of Ionic Liquid Combustion at High Pressure," *Spring Technical Meeting the Central States Section of the Combustion Institute*, 2012.

[52] R. Amrousse, T. Katsumi, N. Azuma and K. Hori, "Hydroxylammonium Nitrate (Han)-Based Green Propellant as Alternative Energy Resource for Potential Hydrazine Substitution: From Lab Scale to Pilot Plant Scale-Up," *Combustion and Flame*, Vol. 176, No. Supplement C, pp. 334-348, 2017. https://doi.org/10.1016/j.combustflame.2016.11.011

[53] T. Katsumi, T. Inoue, J. Nakatsuka, K. Hasegawa, K. Kobayashi, S. Sawai and K. Hori, "Han-Based Green Propellant, Application, and Its Combustion Mechanism," *Combustion, Explosion, and Shock Waves*, Vol. 48, No. 5, pp. 536-543, 2012. 10.1134/S001050821205005X

[54] S. R. Vosen, "The Burning Rate of Hydroxylammonium Nitrate-Based Liquid Propellants," *Symposium (International) on Combustion*, Vol. 22, No. 1, pp. 1817-1825, 1989. https://doi.org/10.1016/S0082-0784(89)80195-X

[55] S. R. Vosen, "Hydroxylammonium Nitrate-Based Liquid Propellant Combustion-Interpretation of Strand Burner Data and the Laminar Burning Velocity," *Combustion and Flame*, Vol. 82, No. 3, pp. 376-388, 1990. https://doi.org/10.1016/0010-2180(90)90009-G

[56] S. R. Vosen, "Concentration and Pressure Effects on the Decomposition Rate of Aqueous Hydroxylammonium Nitrate Solutions," *Combustion Science and Technology*, Vol. 68, No. 4-6, pp. 85-99, 1989. 10.1080/00102208908924070

[57] B. N. Kondrikov, V. É. Annikov, V. Y. Egorshev and L. T. De Luca, "Burning of Hydroxylammonium Nitrate," *Combustion, Explosion and Shock Waves*, Vol. 36, No. 1, pp. 135-145, 2000. 10.1007/BF02701522

VITA

Alex Jeffrey Mundahl was born in 1994, and grew up in Bloomington, Minnesota. Alex graduated from Thomas Jefferson High School in June of 2012 and started at the Missouri University of Science and Technology in August. During his time as an undergraduate student, Alex participated in multiple extracurricular activities including the high-powered rocket design team, Missouri S&T Satellite Research Team, and undergraduate research. In May of 2016 he received his Bachelor's of Science degree in Aerospace Engineering. The summer of that year, he interned with NASA's Marshall Space Flight Center's Propulsion Academy in Huntsville Alabama. After his internship, he returned to Missouri S&T to begin his graduate studies, and received a Master of Science degree in Aerospace Engineering in May of 2018.